

Quantum quenches from excited states in the Ising chain

Leda Bucciantini¹, Márton Kormos^{1,2}, Pasquale Calabrese¹

¹ *Dipartimento di Fisica dell'Università di Pisa and INFN, 56127 Pisa, Italy*

² *MTA-BME "Momentum" Statistical Field Theory Research Group,
1111 Budapest, Budafoki út 8, Hungary*

Abstract

We consider the non-equilibrium dynamics after a sudden quench of the magnetic field in the transverse field Ising chain starting from excited states of the pre-quench Hamiltonian. We prove that stationary values of local correlation functions can be described by the generalised Gibbs ensemble (GGE). Then we study the full time evolution of the transverse magnetisation by means of stationary phase methods. The equal time two-point longitudinal correlation function is analytically derived for a particular class of excited states for quenches within the ferromagnetic phase, and studied numerically in general. The full time dependence of the entanglement entropy of a block of spins is also obtained analytically for the same class of states and for arbitrary quenches.

1 Introduction

Recent experiments in the field of ultra-cold atoms [1–5] triggered an intense theoretical activity aimed to understand the unitary non-equilibrium evolution of isolated many-body quantum systems. A situation which attracted a lot of interest is that of a sudden quench of a Hamiltonian parameter such as an external magnetic field [6]. The most remarkable results that emerged from these theoretical and experimental investigations are probably the following two: (i) there is a light-cone like spreading of correlations following a quantum quench [3, 7–10] and (ii) expectation values of *local* observables generically approach stationary values at late times in the thermodynamic limit, although the whole system is always in a pure state.

Rather amazingly, these stationary values can be predicted by a statistical ensemble without solving the complicated non-equilibrium dynamics. For non-integrable models the appropriate statistical ensemble is expected to be the standard Gibbs one with an effective temperature fixed by the value of the energy in the initial state [11]. For integrable models, the existence of non-trivial local conservation laws strongly constrains the dynamics and the stationary values are expected to be described by a generalised Gibbs ensemble (GGE) [12]. The most convincing evidence supporting this scenario comes from the exact solution of models that can be mapped to free fermions or bosons for which the full dynamics can be obtained analytically. Among these models a crucial role has been played by the transverse field Ising chain which is probably the most intensively investigated model in the quench literature [13–30], although many other free-like models have been studied as well. [31–39]. For integrable interacting models, i.e. with a non-trivial scattering matrix between quasi-particle excitations, the exact solution of the quench dynamics is still an outstanding problem [40], but recently it has been possible in some instances to construct the GGE and compute explicitly a few observables [40–56] and also to check these predictions numerically [56]. Clearly, for non-integrable models the evidence comes only from numerical [57–70] or experimental [1, 2] investigations.

However, most of (if not all) these studies focused on the evolution starting from the ground-state of a given pre-quench Hamiltonian. While these initial states should include all the most relevant experimental situations, it is natural to wonder how general the conclusions drawn on their basis are. Indeed, ground states of local Hamiltonians are not at all generic because their entanglement entropy (i.e. the von Neumann entropy of the reduced density matrix of a subsystem) satisfies an area law [71] (i.e. it scales with the area of the surface of the subsystem) or at most it has multiplicative logarithmic corrections, while generic states satisfy a volume law. This important difference is at the heart of the machinery of the so-called tensor network techniques used to effectively simulate many-body quantum systems (see e.g. Refs. [72] as reviews). Somewhat more general conclusions can be drawn by considering a quantum quench in which the initial state is not a ground-state, but an *excited state of the pre-quench Hamiltonian*, which generically follows a volume law for the entanglement entropy [73] rather than an area law.

In order to give a first answer to this question, in this paper we consider the quench dynamics in the prototype of the models mappable to free fermions, namely the transverse

field Ising chain, which, in spite of its simplicity and the fact that it is exactly solvable, represents a crucial paradigm for quantum critical behaviour. Furthermore, while the model admits a representation in terms of free fermions, the spin variables are non-local with respect to the fermionic degrees of freedom, a property which renders it less trivial than free particle systems and, at the same time, an ideal testing ground for studying the relaxation for which locality is an essential feature.

The manuscript is organised as follows. In Sec. 2 we report all the preliminary information to set up the calculations, i.e. we introduce the model, its diagonalisation, the quench protocol and the observables we will study. In Sec. 3 we show that in the long time limit (taken after the thermodynamic one) the system can be described by a GGE. In Sec. 4 we study the time evolution of the transverse magnetisation, while in the following Sec. 5 we consider the two-point longitudinal correlation function. In Sec. 6 we turn to the time evolution of the entanglement entropy. In the last section we draw our conclusions and in two appendices we report some additional technical details.

2 The model, the quench protocol, and the observables

We consider here the non-equilibrium dynamics of the transverse field Ising chain with Hamiltonian

$$H_I = -\frac{1}{2} \sum_{j=1}^N [\sigma_j^x \sigma_{j+1}^x + h \sigma_j^z], \quad (1)$$

where σ_m^μ , $\mu = x, y, z$ is the Pauli matrix at site m of the chain, h is the transverse field, and we impose periodic boundary conditions $\sigma_{N+1}^\mu = \sigma_1^\mu$. The transverse field Ising chain is a crucial paradigm of quantum phase transitions [74] because at zero temperature and in the thermodynamic limit $N \rightarrow \infty$ it exhibits ferromagnetic ($h < 1$) and paramagnetic ($h > 1$) phases, separated by a quantum critical point at $h_c = 1$.

2.1 The diagonalisation of the Hamiltonian

The diagonalisation of Hamiltonian (1) is presented in several textbooks (see e.g. [74]), but we repeat it here to make the paper self consistent. The first step in diagonalising the Hamiltonian (1) is to introduce a set of spinless fermion annihilation and creation operators through the *non-local* Jordan-Wigner transformation

$$c_l = \left(\prod_{m<l} \sigma_m^z \right) \frac{\sigma_l^x - i\sigma_l^y}{2}, \quad c_l^\dagger = \left(\prod_{m<l} \sigma_m^z \right) \frac{\sigma_l^x + i\sigma_l^y}{2}, \quad (2)$$

where the operators c_l, c_l^\dagger satisfy anti-commutation relation

$$\{c_l^\dagger, c_m\} = \delta_{lm}, \quad \{c_l, c_m\} = 0. \quad (3)$$

Then the Fourier modes d_k are defined as

$$d_k = \frac{1}{\sqrt{N}} \sum_{j=1}^N c_j e^{-i(2\pi k j)/N}. \quad (4)$$

Since the transformation is unitary, also the d_k operators satisfy anti-commutation relations. In terms of d_k operators, the Hamiltonian is

$$H_I = \sum_k \left(\left[h - \cos \frac{2\pi k}{N} \right] d_k^\dagger d_k - \frac{i}{2} \sin \frac{2\pi k}{N} \left[d_{-k} d_k + d_{-k}^\dagger d_k^\dagger \right] - \frac{h}{2} \right), \quad (5)$$

where the sum over the modes k runs over integers or half-integers depending on the parity of the fermion number, see e.g. the Appendix of Ref. [24] for a detailed discussion. This is however superfluous for our goals since we will only consider the thermodynamic limit in which the momentum becomes continuous.

It is now necessary to apply one more unitary transformation to cast the Hamiltonian in a diagonal form: the transformation is a Bogoliubov rotation which takes the fermionic operators d_k, d_k^\dagger to the new ones b_k, b_k^\dagger

$$b_k^\dagger = u_k d_k^\dagger + i v_k d_{-k}, \quad b_k = u_k d_k - i v_k d_{-k}^\dagger, \quad (6)$$

where the coefficients u_k and v_k are chosen in such a way as to make H_I diagonal

$$u_k = \cos(\theta_k/2), \quad v_k = \sin(\theta_k/2), \quad (7)$$

and the angle θ_k is defined by the relation

$$\tan \theta_k = \frac{\sin(2\pi k/N)}{\cos(2\pi k/N) - h}. \quad (8)$$

Again, the unitarity of the transformation ensures the validity of the usual anti-commutation relation for the b operators. Moreover, the characteristic of (6) of mixing only the modes k and $-k$ of the operators d allows us to re-write the Bogoliubov transformation in a more compact way as a rotation in a 2×2 Hilbert space

$$D_k = R_x(\theta_k) B_k, \quad (9)$$

where D_k and B_k are the two-component vectors

$$B_k = \begin{pmatrix} b_k \\ b_{-k}^\dagger \end{pmatrix}, \quad D_k = \begin{pmatrix} d_k \\ d_{-k}^\dagger \end{pmatrix}, \quad (10)$$

and the matrix $R_x(\alpha)$ is a special case of

$$R_\mu(\alpha) = \cos \frac{\alpha}{2} + i \sigma^\mu \sin \frac{\alpha}{2}. \quad (11)$$

The Hamiltonian can be written in terms of the Bogoliubov quasi-particles as

$$H_I = \sum_k \epsilon_k \left(b_k^\dagger b_k - \frac{1}{2} \right), \quad (12)$$

where the one-particle dispersion relation is

$$\epsilon_k = \sqrt{\left(h - \cos \frac{2\pi k}{N} \right)^2 + \sin^2 \left(\frac{2\pi k}{N} \right)}. \quad (13)$$

In the thermodynamic limit, the momentum $\varphi_k = 2\pi k/N$ becomes a continuous variable φ living in the interval $\varphi \in [-\pi, \pi]$. In the following we will often use k instead of φ , being sure that it will always be clear whether we refer to continuous or discrete momenta.

2.1.1 Other useful fermionic operators

For the calculation of correlation functions it is convenient to introduce some other sets of fermionic operators. First, we introduce the Majorana fermions

$$A_j^x = c_j^\dagger + c_j, \quad A_j^y = i(c_j - c_j^\dagger) \quad (14)$$

which satisfy the algebra

$$\{A_l^x, A_n^x\} = 2\delta_{ln}, \quad \{A_l^y, A_n^y\} = 2\delta_{ln}, \quad \{A_l^x, A_n^y\} = 0. \quad (15)$$

While the spin operator σ_n^z is local in terms of these Majorana fermions, $\sigma_n^z = iA_n^y A_n^x$, the operator σ_n^x has the non-local representation

$$\sigma_n^x = \prod_{j=1}^{n-1} (iA_j^y A_j^x) A_n^x, \quad (16)$$

which, as we shall see, is particularly useful in the calculation of real space correlation functions and the entanglement entropy.

The operators A_j^x and A_j^y can be collected together in two different ways. On the one hand, one can introduce a single set of operators at the price of doubling their number per site in the following way

$$A_{2j-1} = A_j^y, \quad A_{2j} = A_j^x, \quad (17)$$

and they satisfy the algebra

$$\{A_a, A_b\} = 2\delta_{ab}. \quad (18)$$

On the other hand, A_j^x and A_j^y can be collected in a two-component vector operator

$$\Omega_j = \begin{pmatrix} iA_j^y \\ A_j^x \end{pmatrix}. \quad (19)$$

We will denote the Fourier transform of A_j^x with ω_k^+ and the Fourier transform of iA_j^y with ω_k^- , and, with a slight abuse of notation, we will denote the Fourier transform of the vector (19) simply as Ω_k :

$$\Omega_k = \begin{pmatrix} \omega_k^- \\ \omega_k^+ \end{pmatrix} = \frac{1}{\sqrt{N}} \sum_{j=1}^N e^{-i(2\pi kj)/N} \begin{pmatrix} iA_j^y \\ A_j^x \end{pmatrix}. \quad (20)$$

2.2 The exact spectrum

The ground state of H_I is the vacuum of Bogoliubov operators, i.e. it is annihilated by all b_k . Its energy is $E_{GS} = -\frac{1}{2} \sum_k \epsilon_k$. However, the exact diagonalisation of the model gives not only the ground state properties but all the eigenstates and their energies. In the basis of free fermions, the excited states are classified according to the occupation numbers of the single-particle basis. An eigenstate can be then written as

$$|m_k\rangle \equiv \prod_k (b_k^\dagger)^{m_k} |0\rangle, \quad \text{with energy } E_{m_k} - E_{GS} = \sum_k m_k \epsilon_k, \quad (21)$$

where $m_k = 0, 1$ is a characteristic function of the state representing the set of occupied momenta, i.e. $m_k = 1$ if the momentum k is occupied and $m_k = 0$ if not. All observables can be written in terms of the characteristic function as for example the energy in Eq. (21). While in finite system the characteristic function can assume only the values 0 and 1, in the thermodynamic limit it becomes an arbitrary function $m(\varphi)$ of $\varphi \in [-\pi, \pi]$ with the restriction to be in the interval $[0, 1]$. This function $m(\varphi)$ is a coarse-grained version of m_k , see e.g. [73] for specific examples. The ground state corresponds to $m_k = 0$ for every k .

2.3 The quench protocol

The time dependence of the system after a quench of the transverse field starting from the ground state has been studied extensively in a series of works, as reported in the introduction. Here we are interested in the case when the initial state is an excited state of the pre-quench Hamiltonian, i.e. for $t < 0$ the system is in an excited state of the Hamiltonian H_I with field equal to h_0 . At time $t = 0$ the value of the field is suddenly quenched to $h \neq h_0$ and all the following time evolution is governed by this new Hamiltonian. We will denote by b'_k and b_k the fermionic mode operators that diagonalise the Hamiltonian with h_0 and h , respectively. Similarly, primed symbols will be used to denote all pre-quenched operators and variables while not-primed ones for post-quench operators and variables. The initial state is then one of those in Eq. (21) for the pre-quench Hamiltonian, i.e.

$$|\Psi_0\rangle = |m_k\rangle = \prod_k (b'_k)^\dagger)^{m_k} |0\rangle. \quad (22)$$

As already discussed this state is fully specified by the characteristic function $m_k = 0, 1$ (in finite systems). The time dependent state is given by

$$|\Psi_0(t)\rangle = e^{-iH_I t} |\Psi_0\rangle, \quad (23)$$

with H_I being the post-quench Hamiltonian with transverse field h .

We point out that even if the states $|m_k\rangle$ are a basis for the many-body Hilbert space, they do not represent the most generic excited state because the spectrum of the Ising chain is highly degenerate and linear combination of degenerate states are still eigenstates, but they cannot be written as (21). One property of the states $|m_k\rangle$ is that they do not break the Z_2 symmetry of the Hamiltonian even in the ferromagnetic phase, unless $m_k = 0$ i.e. in the ground state.

The relation between the pre- and post-quench Bogoliubov operators is given by the combination of the two Bogoliubov rotations in Eq. (6) with angles θ_k and $-\theta'_k$ (i.e. post- and pre-quench Bogoliubov angles, respectively). Thus the overall rotation is

$$B'_k = R_x(\theta_k - \theta'_k)B_k = R_x(\Delta_k)B_k, \quad (24)$$

where we defined $\Delta_k \equiv \theta_k - \theta'_k$. Being Δ_k the main quench variable entering in all the following calculations and results, it is worth writing explicitly its form in terms of h and h_0 :

$$\cos \Delta_k = \frac{hh_0 - (h + h_0) \cos \varphi_k + 1}{\sqrt{1 + h^2 - 2h \cos(\varphi_k)} \sqrt{1 + h_0^2 - 2h_0 \cos(\varphi_k)}}. \quad (25)$$

2.4 Observables, Relaxation and Generalised Gibbs ensemble

The most important observable in the study of quantum quenches is the reduced density matrix ρ_A of a block A built with ℓ contiguous spins. Indeed from ρ_A all the correlation functions local within A can be obtained. Since the system is in a pure state $|\Psi_0(t)\rangle$ at any time, the density matrix of the entire system is

$$\rho(t) = |\Psi_0(t)\rangle\langle\Psi_0(t)|. \quad (26)$$

The reduced density matrix of a subsystem A is defined as

$$\rho_A(t) = \text{Tr}_{\bar{A}}(\rho(t)), \quad (27)$$

where \bar{A} is the complement of A . The importance of ρ_A stems from the fact that it is the quantity which generically displays a stationary behaviour described by some statistical ensemble, while the full density matrix $\rho(t)$ always corresponds to a pure state with zero entropy.

More precisely, following Refs. [25,32] it is usually said that a system reaches a stationary state if a long time limit of the reduced density matrix exists, i.e. if the limit

$$\lim_{t \rightarrow \infty} \rho_A(t) = \rho_A(\infty) \quad (28)$$

exists. This is described by a given statistical (mixed state) ensemble with full density matrix ρ_E if its reduced density matrix restricted to A equals $\rho_A(\infty)$, i.e. if for $\rho_{A,E} = \text{Tr}_{\bar{A}}(\rho_E)$ and for any finite subsystem A

$$\rho_A(\infty) = \rho_{A,E}. \quad (29)$$

In particular, this implies that arbitrary *local* multi-point correlation functions within subsystem A can be evaluated as averages within the ρ_E . By no means this implies that ρ_E equals the full density matrix of the system which is clearly impossible being the former a mixed state and the latter a pure one.

When a system thermalises, ρ_E is the standard Gibbs distribution $\rho_E \propto e^{-\beta H}$ and this is expected to be the case when the model is non-integrable. However, for an integrable model, the proper statistical ensemble describing the system for long time is a generalised Gibbs ensemble (GGE) rather than a thermal one. The density matrix of the GGE is defined as [12]

$$\rho_{\text{GGE}} = \frac{e^{-\sum_n \lambda_n I_n}}{Z}, \quad (30)$$

where I_n is set of commuting integrals of motion, i.e. $[I_n, I_m] = 0$, and Z is a normalisation constant $Z = \text{Tr} e^{-\sum_n \lambda_n I_n}$. It is important for a proper definition of GGE to specify which conserved charges enter in the GGE density matrix above. It has been understood recently [21, 25] that only *local* integrals of motion should be used in Eq. (30) if we are interested in the expectation values of *local* observables such as the reduced density matrix.

While in general it is a formidable task to calculate a reduced density matrix even for an integrable system, in the case of a model that can be mapped to free fermions it is a rather straightforward application of the Wick theorem to write it in terms of only two-point correlators of fermions. To this aim, let us first introduce the *correlation matrix* of Majorana fermions with the definition

$$\langle A_m A_n \rangle = \delta_{mn} + i\Pi_{mn}. \quad (31)$$

For ℓ consecutive fermions (2ℓ Majoranas), using explicitly the periodicity of the chain, this matrix has the block structure

$$\Pi = \begin{bmatrix} \Pi_0 & \Pi_{-1} & \dots & \Pi_{1-\ell} \\ \Pi_1 & \Pi_0 & \dots & \dots \\ \dots & \dots & \dots & \dots \\ \Pi_{\ell-1} & \dots & \dots & \Pi_0 \end{bmatrix}, \quad (32)$$

where the Π_a 's are 2×2 matrices with entries equal to the correlations of Majorana fermions, which explicitly are

$$\delta_{n0} - i\Pi_n = \begin{pmatrix} \langle A_{2l-1} A_{2(l+n)-1} \rangle & \langle A_{2l-1} A_{2(l+n)} \rangle \\ \langle A_{2l} A_{2(l+n)-1} \rangle & \langle A_{2l} A_{2(l+n)} \rangle \end{pmatrix} = \begin{pmatrix} \langle A_l^y A_{l+n}^y \rangle & \langle A_l^y A_{l+n}^x \rangle \\ \langle A_l^x A_{l+n}^y \rangle & \langle A_l^x A_{l+n}^x \rangle \end{pmatrix}, \quad \forall l, \quad (33)$$

where the correlations can clearly be taken to start from an arbitrary site l . Because of its periodic structure, the matrix Π turns out to be a block Toeplitz matrix, i.e. its constituent 2×2 blocks depend only on the difference between row and column indices of Π .

We can now use Wick's theorem to construct all correlation functions in the Ising chain. As shown in Refs. [75, 76], the matrix Π determines entirely the reduced density matrix of the block A of ℓ contiguous fermions in the chain (and hence spins, because contiguous spins

are mapped to contiguous fermions, see Eq. (16)), with a final result that can be written in the compact way [75, 77]

$$\rho_A = \frac{1}{2^\ell} \sum_{\mu_l=0,1} \left\langle \prod_{l=1}^{2\ell} A_l^{\mu_l} \right\rangle \left(\prod_{l=1}^{2\ell} A_l^{\mu_l} \right)^\dagger \propto e^{A_l W_{lm} A_m / 4}, \quad (34)$$

where [77]

$$\tanh \frac{W}{2} = i\Pi. \quad (35)$$

Given ρ_A we can calculate any local correlation function with support in A . Very importantly, because of this direct relation between reduced density matrix and correlation matrix, it is sufficient to prove that the two ensembles or states have the same correlation matrix in order to prove that they are equal. This is an immense simplification because while ρ_A has $2^\ell \times 2^\ell$ elements, Π has only $2\ell \times 2\ell$ elements.

From the reduced density matrix, another fundamental observable is easily constructed, namely the entanglement entropy which is the von Neumann entropy of ρ_A ,

$$S_A = -\text{Tr} \rho_A \ln \rho_A. \quad (36)$$

Using again Wick's theorem [75], S_A can be related to the eigenvalues of the matrix Π . Indeed, denoting the eigenvalues of Π as $\pm i\nu_m$, $m = 1 \dots \ell$ (being Π an antisymmetric matrix, its eigenvalues are purely imaginary complex conjugate pairs), the entanglement entropy is [75]

$$S = \sum_{m=1}^{\ell} H(\nu_m), \quad \text{where} \quad H(x) = -\frac{1+x}{2} \ln \left(\frac{1+x}{2} \right) - \frac{1-x}{2} \ln \left(\frac{1-x}{2} \right). \quad (37)$$

Apart from the reduced density matrix, we will also consider the transverse magnetisation

$$m^z(t) = \langle \sigma_i^z \rangle = \langle iA_i^x A_i^y \rangle, \quad (38)$$

and the two-point function of the order parameter at a distance ℓ

$$\rho^{xx}(\ell) \equiv \langle \sigma_n^x \sigma_{\ell+n}^x \rangle. \quad (39)$$

While m^z is local within fermions, $\rho^{xx}(\ell)$ is not. However, in computing $\rho^{xx}(\ell)$ only the string of Majorana fermions between sites n and $n + \ell$ matters and thus it takes the form [13, 74]

$$\rho^{xx}(\ell) = \left\langle \prod_{j=n}^{\ell+n-1} (-iA_j^y A_{j+1}^x) \right\rangle. \quad (40)$$

By means of Wick's theorem [13, 74], $\rho^{xx}(\ell)$ can be written as the Pfaffian of a skew symmetric $2\ell \times 2\ell$ matrix

$$\rho^{xx}(\ell) = \text{pf}(\Gamma), \quad (41)$$

where Γ is given by

$$\Gamma = \begin{bmatrix} \Gamma_0 & \Gamma_{-1} & \dots & \Gamma_{1-\ell} \\ \Gamma_1 & \Gamma_0 & \dots & \dots \\ \dots & \dots & \dots & \dots \\ \Gamma_{\ell-1} & \dots & \dots & \Gamma_0 \end{bmatrix}, \quad (42)$$

where

$$\delta_{n0} - i\Gamma_n = \begin{pmatrix} \langle A_l^y A_{l+n}^y \rangle & \langle A_l^x A_{l+n-1}^y \rangle \\ \langle A_l^y A_{l+n+1}^x \rangle & \langle A_l^x A_{l+n}^x \rangle \end{pmatrix}, \quad \forall l. \quad (43)$$

Notice that although the matrices Γ and Π in Eq. (33) look very similar and they have the same block-diagonal elements, the off-diagonal ones are different since the second operator is shifted by ± 1 . We note that in the literature the two matrices are often denoted by the same symbol and it is very easy to mix them up.

3 The infinite time limit and the generalised Gibbs ensemble

In this section we consider the infinite time limit of the reduced density matrix ρ_A of a subsystem A composed of ℓ contiguous spins. To analyse ρ_A , we first consider the time evolution of the long time limit of its building blocks, that, according to Eq. (34), are the two-point real-space correlation functions of fermions.

3.1 Time evolution of the fermionic two-point function

The Bogoliubov rotations diagonalising the pre- and post-quench Hamiltonians only couple modes with opposite momenta, cf. Eq. (9). It is then convenient to cast the two-point correlation functions of pre-quench Bogoliubov modes in the 2×2 matrix

$$\begin{aligned} \langle \Psi_0 | B'_k B'_k{}^\dagger | \Psi_0 \rangle &= \begin{pmatrix} \langle b'_k b'_k{}^\dagger \rangle & \langle b'_k b'_{-k} \rangle \\ \langle b'_{-k}{}^\dagger b'_k{}^\dagger \rangle & \langle b'_{-k}{}^\dagger b'_{-k} \rangle \end{pmatrix} = \begin{pmatrix} 1 - m_k & 0 \\ 0 & m_{-k} \end{pmatrix} \\ &= \frac{1}{2} [\sigma_z (1 - m_k - m_{-k}) + \mathbb{I} (1 - m_k + m_{-k})], \end{aligned} \quad (44)$$

in which $|\Psi_0\rangle$ is the initial state specified by the function m_k as in Eq. (22). Combining the two Bogoliubov rotations for pre- and post-quench Hamiltonian as in Eq. (24), we write the expectation value of post-quench Bogoliubov operators in the initial state as

$$\begin{aligned} \langle \Psi_0 | B_k B_k{}^\dagger | \Psi_0 \rangle &= \langle \Psi_0 | R_x(-\Delta_k) B'_k B'_k{}^\dagger R_x^\dagger(-\Delta_k) | \Psi_0 \rangle \\ &= \begin{pmatrix} \sin^2 \frac{\Delta_k}{2} m_{-k} + \cos^2 \frac{\Delta_k}{2} (1 - m_k) & -\frac{i}{2} \sin \Delta_k (-1 + m_{-k} + m_k) \\ \frac{i}{2} \sin \Delta_k (-1 + m_{-k} + m_k) & \cos^2 \frac{\Delta_k}{2} m_{-k} + \sin^2 \frac{\Delta_k}{2} (1 - m_k) \end{pmatrix}, \end{aligned} \quad (45)$$

which is the initial condition for the fermionic two-point functions. The time evolution can be worked out in the Heisenberg picture where the post-quench operators $B_k(t)$ evolve according to the Hamiltonian (12), so $B_k(t) = U_k(t)B_k(0)$, where $U_k(t)$ is the restriction of the time evolution operator to the subset of the Hilbert space with momenta k and $-k$, i.e.

$$U_k(t) = \begin{pmatrix} e^{-i\epsilon_k t} & 0 \\ 0 & e^{i\epsilon_k t} \end{pmatrix} = R_z(-2\epsilon_k t). \quad (46)$$

It is now possible to evaluate the expectation value of expressions bilinear in the fermions c_i and c_i^\dagger at any time. In order to do so, it is enough to invert Eq. (4) and express the d operators in terms of b which evolve according to Eq. (46). From $c_l = \sum_k e^{i2\pi kl/N} (u_k b_k + i v_k b_{-k}^\dagger) / \sqrt{N}$, we can write

$$c_l(t) = \frac{1}{\sqrt{N}} \sum_k e^{i2\pi kl/N} \left(u_k b_k(t) + i v_k b_{-k}^\dagger(t) \right) = \frac{1}{\sqrt{N}} \sum_k e^{i2\pi kl/N} \left(u_k e^{-i\epsilon_k t} b_k + i v_k e^{i\epsilon_k t} b_{-k}^\dagger \right), \quad (47)$$

and similarly for $c_l^\dagger(t)$. Hence from Eq. (20) we obtain for the Fourier transform of Majorana operators

$$\omega_k^+(t) = e^{i\theta_k/2} \left(b_k e^{-i\epsilon_k t} + b_{-k}^\dagger e^{i\epsilon_k t} \right), \quad \omega_k^-(t) = e^{-i\theta_k/2} \left(b_{-k}^\dagger e^{i\epsilon_k t} - b_k e^{-i\epsilon_k t} \right). \quad (48)$$

The vector operator $\Omega_k(t)$ has the form

$$\Omega_k(t) = \begin{pmatrix} -e^{-i(\theta_k/2 + \epsilon_k t)} & e^{i(-\theta_k/2 + \epsilon_k t)} \\ e^{i(\theta_k/2 - \epsilon_k t)} & e^{i(\theta_k/2 + \epsilon_k t)} \end{pmatrix} B_k. \quad (49)$$

Thus

$$\begin{aligned} \langle \Omega_k(t) \Omega_k^\dagger(t) \rangle &= \langle \Psi_0 | \begin{pmatrix} -\omega_k^-(t) \omega_{-k}^-(t) & \omega_k^-(t) \omega_{-k}^+(t) \\ -\omega_k^+(t) \omega_{-k}^-(t) & \omega_k^+(t) \omega_{-k}^+(t) \end{pmatrix} | \Psi_0 \rangle \\ &= \begin{pmatrix} 1 + m_k^A - m_k^S \sin 2t\epsilon_k \sin \Delta_k & m_k^S e^{-i\theta_k} (\cos \Delta_k - i \cos 2t\epsilon_k \sin \Delta_k) \\ m_k^S e^{i\theta_k} (\cos \Delta_k + i \cos 2t\epsilon_k \sin \Delta_k) & 1 + m_k^A + m_k^S \sin 2t\epsilon_k \sin \Delta_k \end{pmatrix}, \end{aligned} \quad (50)$$

where we defined

$$m_k^S \equiv m_{-k} + m_k - 1, \quad (51)$$

$$m_k^A \equiv m_{-k} - m_k, \quad (52)$$

which stand for the even and odd part of m_k respectively. It is straightforward to check that when m_k and m_{-k} are set to zero this expression reduces to the one obtained in the case when the initial state is the ground state of the initial Hamiltonian [16, 25]. Note that if $m_k^S = 0$ then Eq. (50) is constant in time, which is a manifestation of the fact that if $m_k^S = 0$ for any k the state is not only an eigenstate of the pre-quench Hamiltonian but also of the post-quench one. We will define the states with $m_k^A = 0$ as *parity invariant states* (PIS) in which all the positive and negative momentum modes are populated with the same weights.

Note that all the PIS have zero momentum, but the condition for PIS is more restrictive than that. We will refer to the states with $m_k^A \neq 0$ for some k as *non parity invariant states* (NPIS).

Equation (50) is the final expression for the two-point function of fermions in momentum space from which, by Fourier transform, the one for real-space fermions given by Eq. (33) can be straightforwardly obtained. As a usual feature of free systems, each momentum mode oscillates in time with typical frequency proportional to ϵ_k . However, when taking the Fourier transform, in the *thermodynamic limit* the various modes interfere in a destructive way and their long-time expectation is the time-average of the expression above, i.e.

$$\overline{\langle \Omega_k(t) \Omega_k^\dagger(t) \rangle} = \begin{pmatrix} 1 + m_k^A & m_k^S e^{-i\theta_k} \cos \Delta_k \\ m_k^S e^{i\theta_k} \cos \Delta_k & 1 + m_k^A \end{pmatrix}. \quad (53)$$

Thus, in order to show that the reduced density matrix attains a stationary behaviour described by GGE, it is sufficient to show that the GGE prediction for $\langle \Omega_k \Omega_k^\dagger \rangle$ equals Eq. (53). By no means this implies that $\langle \Omega_k(t) \Omega_k^\dagger(t) \rangle$ has a long-time limit, on the contrary, it oscillates forever as a consequence of the fact that the state is pure for any time and the Hamiltonian governing the evolution is diagonal in the modes.

3.2 GGE expectation value of the fermionic two-point function

The GGE density matrix for the full system is given by Eq. (30) constructed with the local integrals of motion. However, it has been shown that for the transverse field Ising chain the post-quench occupation number operators

$$n_k = b_k^\dagger b_k, \quad (54)$$

although non-local quantities, can be written as linear combinations of the local integrals of motion [27] (see also the next subsection). Thus the GGE density matrix constructed with local integrals of motion and the one constructed with n_k are equivalent. We will then consider

$$\rho_{\text{GGE}} = \frac{e^{-\sum_k \lambda_k n_k}}{Z}, \quad (55)$$

where we use the same symbols for the Lagrange multipliers λ_k and λ_n in Eq. (30) since we will never use the two concomitantly. The λ_k are fixed by matching the expectation values of the occupation numbers with their values in the initial state, i.e. imposing

$$\langle \Psi_0 | b_k^\dagger b_k | \Psi_0 \rangle = \text{Tr}[\rho_{\text{GGE}} b_k^\dagger b_k]. \quad (56)$$

The left-hand-side of this equation can be read out from Eq. (45)

$$\langle n_k \rangle = \langle \Psi_0 | b_k^\dagger b_k | \Psi_0 \rangle = 1 - \sin^2 \left(\frac{\Delta_k}{2} \right) m_{-k} - \cos^2 \left(\frac{\Delta_k}{2} \right) (1 - m_k), \quad (57)$$

while the right-hand-side is

$$\langle n_k \rangle = \text{Tr}[\rho_{\text{GGE}} b_k^\dagger b_k] = \frac{1}{1 + e^{\lambda_k}}. \quad (58)$$

Equating the two expressions we get the equation determining λ_k :

$$\frac{1}{1 + e^{\lambda_k}} = 1 - \sin^2\left(\frac{\Delta_k}{2}\right) m_{-k} - \cos^2\left(\frac{\Delta_k}{2}\right) (1 - m_k). \quad (59)$$

The components of $\langle \Omega_k \Omega_k^\dagger \rangle$ can be readily calculated in the GGE, for example

$$\begin{aligned} \langle \omega_k^+ \omega_{-k}^+ \rangle &= \text{Tr}[\rho_{\text{GGE}} \omega_k^+ \omega_{-k}^+] = \frac{1}{Z} \text{Tr}[e^{-\sum_k \lambda_k b_k^\dagger b_k} (1 - b_k^\dagger b_k + b_{-k}^\dagger b_{-k})] \\ &= 1 - \frac{1}{1 + e^{\lambda_k}} + \frac{1}{1 + e^{\lambda_{-k}}} = 1 - \langle n_k \rangle + \langle n_{-k} \rangle = 1 + m_{-k} - m_k = 1 + m_k^A. \end{aligned} \quad (60)$$

Performing similar calculations for the other three elements of the matrix $\langle \Omega_k \Omega_k^\dagger \rangle$ we finally get

$$\langle \Omega_k \Omega_k^\dagger \rangle_{\text{GGE}} = \begin{pmatrix} 1 + m_k^A & m_k^S e^{-i\theta_k} \cos \Delta_k \\ m_k^S e^{i\theta_k} \cos \Delta_k & 1 + m_k^A \end{pmatrix}, \quad (61)$$

which coincides with Eq. (53). This proves that the GGE two-point functions of fermions at arbitrary distance are equal to the long-time limit of the same two-point function after a quench from an excited state $|m_k\rangle$ of the initial Hamiltonian. Since the reduced density matrix can be constructed solely from the fermionic two-point functions as in Eq. (34), this also proves that any local multipoint correlation function of spins and fermions will be described by the GGE for long times.

3.3 Local Conservation laws in the TFIC

It is instructive to have a look at the behaviour of the local conservation laws in the chain in order to check whether they bring any further understanding in the non-equilibrium quench dynamics. In the thermodynamic limit there is an infinite number of local conserved charges which can be written in terms of the post-quench occupation numbers as [27, 78]

$$\begin{aligned} I_n^- &= - \int_{-\pi}^{+\pi} \frac{dk}{2\pi} \sin[(n+1)k] b_k^\dagger b_k, \\ I_n^+ &= \int_{-\pi}^{+\pi} \frac{dk}{2\pi} \cos(nk) \epsilon_k b_k^\dagger b_k, \quad n \geq 0, \end{aligned} \quad (62)$$

where the apex \pm refers to their parity properties: I_n^+ are even and I_n^- are odd under spatial reflections. The expectation values of these conserved charges in the initial state (and in the

subsequent time evolution) is obtained by inserting the expectation value of n_k of Eq. (57) into Eq. (62):

$$\begin{aligned}\langle I_n^- \rangle &= - \int_{-\pi}^{+\pi} \frac{dk}{4\pi} \sin[(n+1)k] m_k^A, \\ \langle I_n^+ \rangle &= \int_{-\pi}^{+\pi} \frac{dk}{4\pi} \cos(nk) \epsilon_k [1 + m_k^S \cos \Delta_k].\end{aligned}\tag{63}$$

Hence $\langle I_n^+ \rangle$ and $\langle I_n^- \rangle$ are both, in general, non-vanishing for an initial excited state. This is different from what happens if the initial state is the ground state of the pre-quench Hamiltonian, when all the parity-odd charges I_n^- vanish. However, $\langle I_n^- \rangle$ is zero every time that $m_k^A = 0$, i.e. for PIS with $m_k = m_{-k}$. This will represent an important class of states for which the calculation of some local observables in the following will be much easier. It is surely interesting to understand whether the increased number of non-zero conservation laws alters somehow the time-dependence of the asymptotic behaviour of local correlation functions.

Finally we would like to emphasise that the $\langle I_n^- \rangle$'s depend only on the initial state and not on the quench parameters, which are entirely contained in the Δ_k angle that instead appears in $\langle I_n^+ \rangle$. The independence of $\langle I_n^- \rangle$ on the Bogoliubov transformation was also pointed out in Refs. [27,28].

4 Transverse magnetisation

The first observable we consider is the transverse magnetisation which is particularly easy to calculate because it has a local expression in terms of fermions, cf. Eq. (38).

In the case when the initial state is the pre-quench ground state the transverse magnetisation is in the thermodynamic limit [13,25]

$$m^z(t) = - \int_{-\pi}^{\pi} \frac{dk}{4\pi} e^{i\theta_k} [\cos \Delta_k - i \sin \Delta_k \cos(2\epsilon_k t)].\tag{64}$$

For an excited state with characteristic function m_k , $m^z(t)$ can be easily found expressing the c_i in terms of the $\omega_k^+(t), \omega_k^-(t)$ and substituting the matrix elements of Eq. (50). After simple algebra we obtain in the thermodynamic limit

$$m^z(t) = \int_{-\pi}^{\pi} \frac{dk}{4\pi} e^{i\theta_k} m_k^S [\cos \Delta_k - i \sin \Delta_k \cos(2\epsilon_k t)],\tag{65}$$

which again reduces to the ground-state evolution in the case $m_k^S = -1$, i.e. $m_k = 0$. Quite remarkably, we have that only the symmetric part of the characteristic function m_k

contributes to the time evolution of the transverse magnetisation and so the odd conserved charges in Eq. (63) have no influence at all on this observable.

Furthermore, the result can be divided into a stationary and a time-dependent part. As for the ground-state case, it is particularly interesting to understand the approach to the stationary value which can be evaluated by a stationary phase approximation. The stationary points are the zeros of $\epsilon'_k = d\epsilon_k/dk$ in the interval $[-\pi, \pi]$, which are $-\pi, 0, \pi$. However, when the characteristic function m_k is not an analytic function in k , possible new extrema of the integration domain need to be taken into account in the calculation. Indeed, these extrema need not coincide with $-\pi, \pi$, as it happens for example in the case in which the initial state excitations m_k are non-zero only in a particular subinterval of $[-\pi, \pi]$.

In the general case under consideration, we have integrals of the form

$$I(t) = \int_a^b dk f(k) e^{itg(k)}, \quad (66)$$

where a and b do not need to coincide with $-\pi$ and π . Notice also that in Eq. (65) the stationary points of $g(k)$ are always zeros of $f(k)$, requiring to go to the second order in stationary phase approach. There are three different classes of extremal points which should be summed up in order to have the complete large time behaviour. Denoting with k_0 each of the points, the three classes are

- 1) The extremal point k_0 is internal to the domain of integration, i.e. $k_0 \in (a, b)$. In this case k_0 must be stationary to be extremal, i.e. $\epsilon'(k_0) = 0$, and then we have

$$I(t) = I_0(t) \equiv e^{itg(k_0)} \left[\frac{f''(k_0)}{2} \frac{\sqrt{\pi}}{2} \frac{1}{(-a')^{3/2}} + O[(-a')^{-5/2}] \right], \quad (67)$$

where $a' = \frac{it}{2} g''(k_0)$. Because of $f(k_0) = 0$ the leading behaviour is $(-a')^{-3/2}$ instead of $(-a')^{-1/2}$.

- 2) The extremal point k_0 is at the boundary of the integration domain, i.e. $k_0 = a$ or b and it is also stationary, i.e. $\epsilon'(k_0) = 0$, in which case we have

$$I(t) = \frac{1}{2} I_0(t). \quad (68)$$

- 3) Finally, the extremal point can be at the boundary of the integration domain, i.e. $k_0 = a$ or b , but it is not stationary i.e. $\epsilon'(k_0) \neq 0$. For $k_0 = a$ and not stationary we have

$$I(t) = -f(a) \frac{e^{itg(a)}}{itg'(a)}, \quad (69)$$

and the same without the minus sign for $k_0 = b$.

It is clear that cases (1) and (2) give a different contribution compared to case (3). Indeed the first two cases generically give a large time behaviour of the type $t^{-3/2}$ (whenever $f''(k_0) \neq 0$, else the contribution would be faster like $t^{-5/2}$), like in the quench from the ground state. The third case instead will generically produce a slower decay of the type t^{-1} (unless $f(a) = 0$, in which case we will have t^{-2}).

For a generic initial state with characteristic function m_k , the general strategy would be the following: (i) divide the integral in Eq. (65) in pieces in which m_k^S is continuous, (ii) treat each of the integrals as in Eq. (66), and finally (iii) sum up all the contributions with the slowest power-law behaviour. In order to show the differences between the various states, we compare the evolution from the ground state with the ones from three representative excited states. We choose the following three states

$$\begin{aligned} m_1(k) &= \theta(k - \pi/2), \\ m_2(k) &= (k/\pi)^2, \\ m_3(k) &= (k + \pi)/(4\pi), \end{aligned} \tag{70}$$

where all $m_a(k)$ are clearly defined in the interval $[-\pi, \pi]$.

For the initial ground state we regain the large time behaviour [25]

$$m_0^z(t) \simeq m_{\text{stat}0}^z - \frac{c(t)}{(hJt)^{3/2}}, \tag{71}$$

where

$$c(t) = \frac{(h - h_0)}{32\sqrt{2}\pi J} \left[\frac{\cos(\pi/4 + 4Jt(1 + h))}{(1 + h_0)\sqrt{1 + h}} + \frac{\sin(\pi/4 + 4Jt|h - 1|)}{|h_0 - 1|\sqrt{|h - 1|}} \right]. \tag{72}$$

For the initial state characterised by $m_1(k)$ we obtain

$$m_1^z(t) \simeq m_{\text{stat}1}^z - \frac{c_{11}(t)}{(hJt)} - \frac{c_{12}(t)}{(hJt)^{3/2}}, \tag{73}$$

where

$$\begin{aligned} c_{11}(t) &= -\frac{(h - h_0)}{16J\pi} \frac{\sin(4Jt\sqrt{1 + h^2})}{\sqrt{(1 + h^2)(1 + h_0^2)}}, \\ c_{12}(t) &= \frac{(h - h_0)}{64J\sqrt{\pi}} \frac{[\sin(4Jt|h - 1|) + \cos 4Jt(h - 1)]}{\sqrt{|h - 1||h_0 - 1|}}. \end{aligned} \tag{74}$$

The leading large time behaviour going like t^{-1} comes from the extrema $\pm\pi/2$ (non-stationary points) while the $t^{-3/2}$ from the $k = 0$ stationary point. Conversely, for the initial states characterised by $m_2(k)$ and $m_3(k)$ we get a $t^{-3/2}$ power law behaviour due to the stationary points $x = 0, \pm\pi$ falling into cases 1) and 2) above, similarly to the ground state but with different calculable coefficients that we do not report here, but are easily obtained from Eqs. (67) and (68).

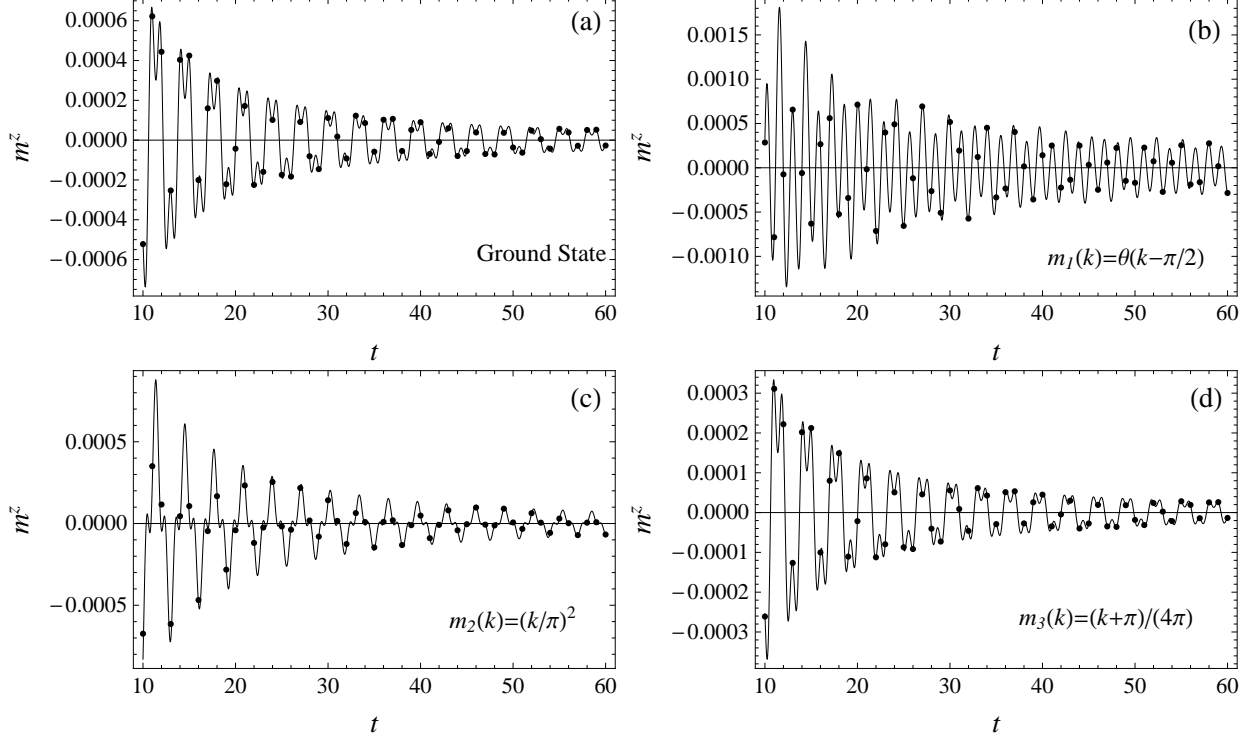


Figure 1: Transverse magnetisation minus its stationary value as a function of time for quenches from $h_0 = 12$ to $h = 2$ for different initial states. The points represent the exact evaluation of the integral in Eq. (65) while the lines are the stationary phase approximation results valid for large time. a) Ground state. b) $m_1(k) = \theta(k - \pi/2)$. c) $m_2(k) = (k/\pi)^2$. d) $m_3(k) = (k + \pi)/(4\pi)$. In all the cases the agreement is excellent for large enough time.

In order to show the reliability and the range of validity of the stationary phase approximations, in Fig. 1 we report the time dependent part of the transverse magnetisation (i.e. we subtract the stationary behaviour). We compare the exact results from the numerical determination of the integral in Eq. (65) with the stationary phase approximation up to order $t^{-3/2}$. It is evident that even for not so-large time the oscillating power-law decay of the stationary phase correctly describes the data. We mention that in the case of Eq. (73) it is important to keep the term $t^{-3/2}$ to describe the data for not too large times.

To conclude this section we would like to emphasise the main difference we have found in the large time behaviour of the transverse magnetisation starting from the ground-state or from excited states of the pre-quench Hamiltonian. For quenches starting from the ground-state we always have a power-law tail of the form $t^{-3/2}$. While several excited states have the same power-law behaviour, this is not true in general. The state with $m_1(k)$ above presents a much slower relaxation going like t^{-1} . We stress that this is not at all an academic state, quite the reverse, it is the most physical among the ones presented above because it has all the modes larger than a given one ($\pi/2$, but this is not essential) occupied. Furthermore by

choosing very particular momentum occupation functions $m(k)$, it is not difficult to cook up quite untypical power-law behaviours: for example, considering $m(k) = \sin^2(k)$, since it vanishes in all the stationary points of the phase $\epsilon(k)$, we obtain a power-law decay like $t^{-5/2}$.

5 Equal-time two point longitudinal correlation function

In this section we investigate the longitudinal spin-spin correlation function between two spins at a distance ℓ at the same time t , i.e.

$$\rho^{xx}(\ell, t) \equiv \langle \Psi_0(t) | \sigma_n^x \sigma_{\ell+n}^x | \Psi_0(t) \rangle. \quad (75)$$

The most interesting regime of this two-point function is the so-called *space-time scaling limit* [21, 24] defined as the limit $t, \ell \rightarrow \infty$ with their ratio t/ℓ kept fixed. In general, the space-time scaling limit does not have to commute with the limit $t \rightarrow 0$ or $t \rightarrow \infty$ either if taken before or after the thermodynamic limit.

The two-point function $\rho^{xx}(\ell, t)$ is the Pfaffian of the $2\ell \times 2\ell$ matrix Γ in Eq. (42) the elements of which are the already calculated two-point fermion functions in Eq. (43). The fermionic correlators in Eq. (43) can be identified looking at Eq. (50), obtaining that the two-by-two constituent blocks have the form

$$\Gamma_n = \begin{pmatrix} h_n & g_n \\ -g_{-n} & f_n \end{pmatrix}, \quad (76)$$

with elements

$$f_n + i\delta_{n0} \equiv i \langle A_j^x A_{j+n}^x \rangle = \frac{i}{N} \sum_k e^{i2\pi kn/N} [1 + m_k^A - m_k^S \sin 2t\epsilon_k \sin \Delta_k], \quad (77)$$

$$h_n + i\delta_{n0} \equiv i \langle A_j^y A_{j+n}^y \rangle = \frac{i}{N} \sum_k e^{i2\pi kn/N} [1 + m_k^A + m_k^S \sin 2t\epsilon_k \sin \Delta_k], \quad (78)$$

$$g_n \equiv i \langle A_j^x A_{j+n-1}^y \rangle = \frac{1}{N} \sum_k e^{i2\pi kn/N} [-m_k^S e^{-ik} e^{i\theta(k)} (\cos \Delta_k - i \cos 2t\epsilon_k \sin \Delta_k)]. \quad (79)$$

Thus in the thermodynamic limit we have

$$\Gamma_n = \begin{pmatrix} h_n & g_n \\ -g_{-n} & f_n \end{pmatrix} = \int_{-\pi}^{\pi} \frac{dk}{2\pi} e^{ikn} \hat{\Gamma}(k), \quad \text{with} \quad \hat{\Gamma}(k) = \begin{pmatrix} h(k) & g(k) \\ -g(-k) & f(k) \end{pmatrix}, \quad (80)$$

with

$$\begin{aligned} f(k) &= i [m_k^A - m_k^S \sin 2t\epsilon_k \sin \Delta_k], \\ h(k) &= i [m_k^A + m_k^S \sin 2t\epsilon_k \sin \Delta_k], \\ g(k) &= -m_k^S e^{-ik} e^{i\theta(k)} (\cos \Delta_k - i \cos 2t\epsilon_k \sin \Delta_k). \end{aligned} \quad (81)$$

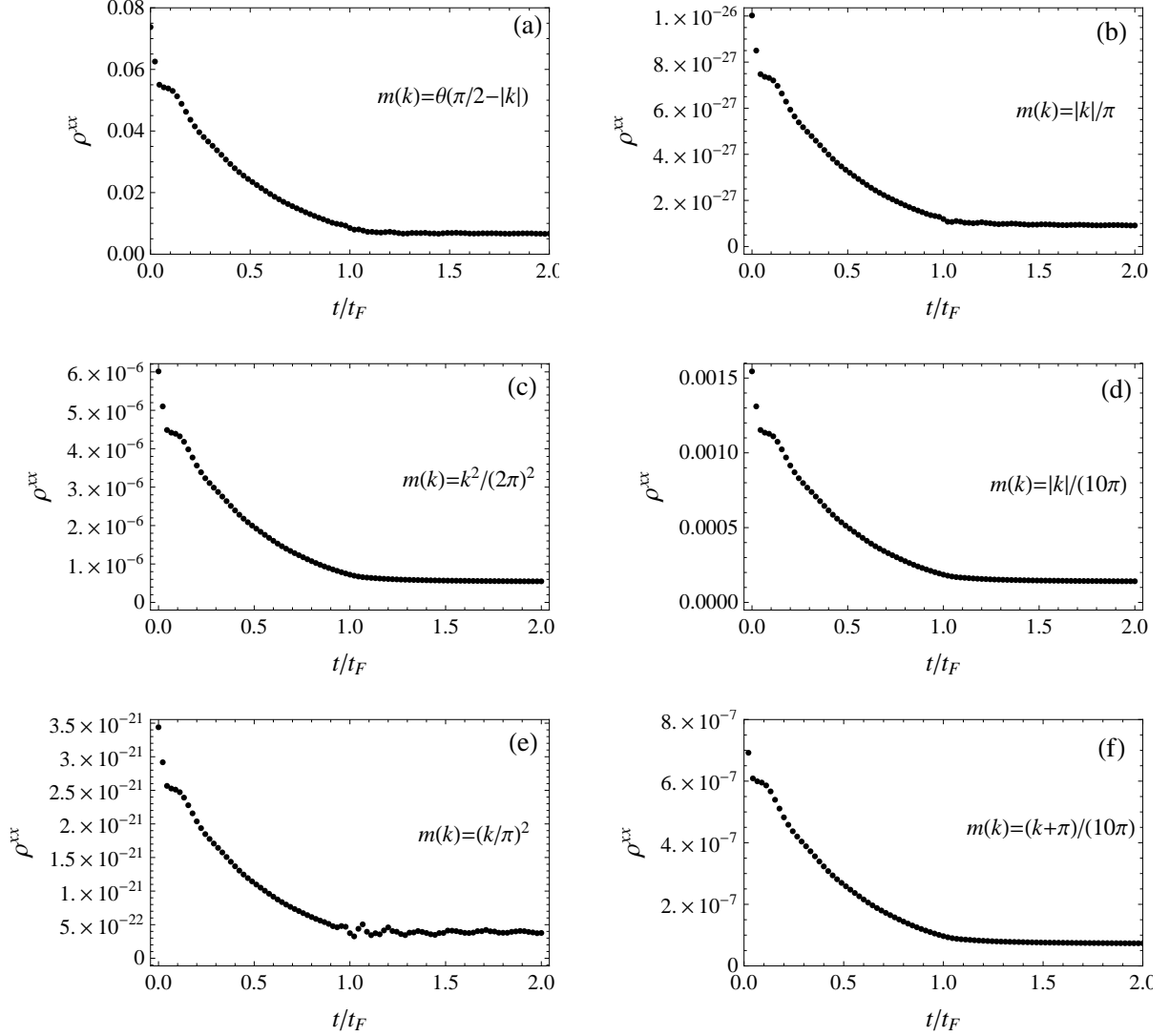


Figure 2: Two-point longitudinal correlation function for $\ell = 60$ as a function of time. All figures refer to quenches from $h_0 = 1/3$ to $h = 2/3$. Each panel corresponds to a different excited state with characteristic function $m(k)$ given by: a) $m(k) = \theta(\pi/2 - |k|)$, b) $m(k) = |k|/\pi$ c) $m(k) = k^2/(2\pi)^2$, d) $m(k) = |k|/(10\pi)$, e) $m(k) = (k/\pi)^2$, f) $m(k) = (k + \pi)/(10\pi)$.

The 2×2 matrix $\hat{\Gamma}(k)$ is called the *block symbol* of the matrix Γ . Since $f(k)$ and $h(k)$ are odd functions of k , the matrix Γ is antisymmetric and of Toeplitz form, as it should be. Notice that when the initial state is the ground state of the pre-quench Hamiltonian $h(k) = -f(k)$, which is also the case every time when $m_k^A = 0$, i.e. $m_k = m_{-k}$.

5.1 Numerical results

We report in this section the numerical results obtained for the longitudinal correlator for various initial excited states. We restrict ourselves to quenches within the ferromagnetic phase, because, as for the ground-state case [21, 24], quenches between the phases and within the paramagnetic phase have a more complicated time dependence. All the following numerical results have been obtained for the quench from $h_0 = 1/3$ to $h = 2/3$, but the conclusions we draw are valid for arbitrary quenches within the ferromagnetic phase. The time evolution of the two-point function $\rho^{xx}(\ell, t)$ is reported in units of the Fermi time t_F , defined as [24]

$$t_F = \frac{\ell}{2v_{\max}}, \quad (82)$$

where v_{\max} is the maximal propagation velocity of the elementary excitations

$$v_{\max} = \max_{k \in [-\pi, \pi]} |\epsilon'_k| = \min[h, 1]. \quad (83)$$

In Fig. 2 we report the obtained numerical results for the correlation function at fixed distance $\ell = 60$. All the data reported in these plots show a quite general behaviour: for $t < t_F$ the correlation function decays exponentially, while for $t > t_F$ it shows a slow relaxation toward the GGE value. This is a manifestation of the light-cone spreading of correlations [7] also for these quenches from excited states. However, not all the initial excited states we analysed behave in this way and for that reason we show it separately in Fig. 3. There we report the time evolution from the state characterised by $m(k) = \theta(k - \pi/2)$ which appears qualitatively different from the others: while for $\ell = 20, 60$ it is similar to the other cases in Fig. 2, for $\ell = 30, 90$ after an initial decay the correlation function displays a sort of plateaux and at $t \sim t_F$ it sets around the GGE value which is reached in an oscillating manner. It is not clear to us what the physical phenomenon behind this behaviour is, but we have observed it only for NPIS (i.e. for $m_k \neq m_{-k}$). Furthermore, the analytic result obtained in the next subsection for PIS shows that they always behave as in Fig. 2. Thus it is natural to believe that the anomalous behaviour in Fig. 3 is due to the non-vanishing odd conservation laws during the time evolution, but how exactly this happens is still to be understood, even because some NPIS behaves like their PIS counterpart as the case (f) in Fig. 2.

Also for the well behaved cases in Fig. 2 there is a fundamental difference compared to the ground-state initial case which is worth mentioning. In equilibrium, all these states are characterised by a vanishing one-point function $\langle \sigma^x \rangle$ explaining why the initial values of the two-point functions in Fig. 2 is always within the range $10^{-1} - 10^{-27}$ (and obviously it goes to zero increasing ℓ), while it was close to 1 for the ground-state quench. Furthermore it also seems that the more excited the state is, the lower is the initial value of two point correlator. This can be seen from Fig. 2 by comparing the initial states in which m_k has the same analytical form but different pre-factor. However, we did not explore this aspect in detail because it is not of direct interest to this manuscript.

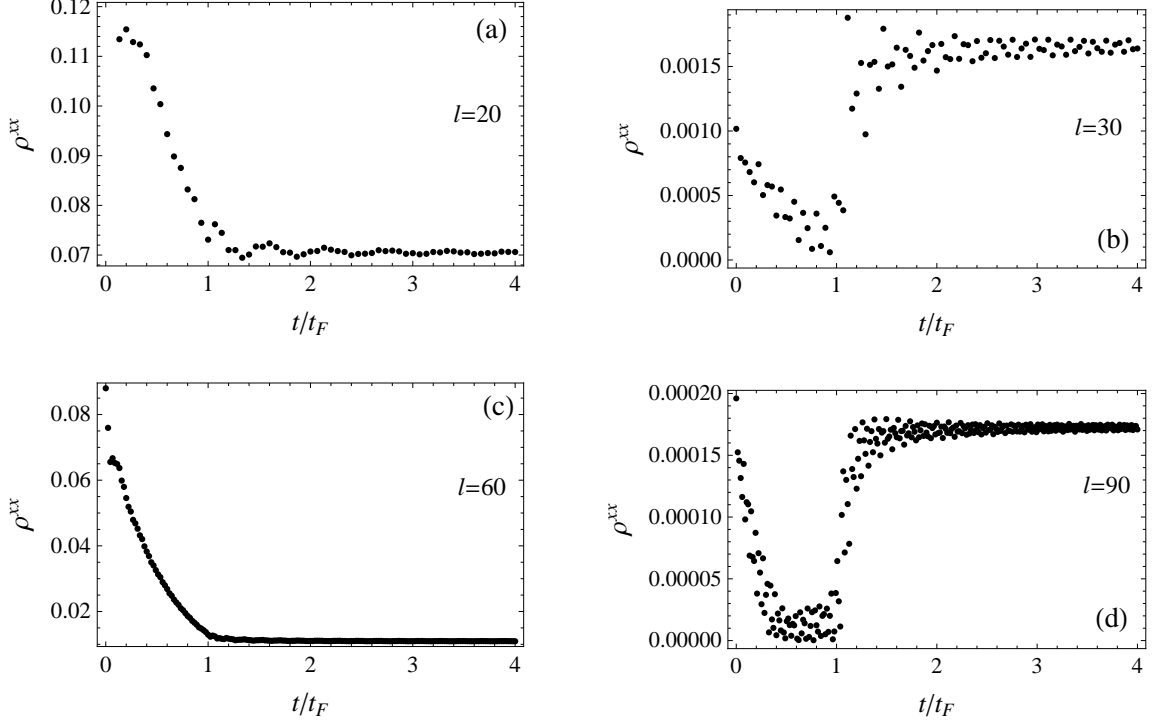


Figure 3: Two-point longitudinal correlation function for the quench from $h_0 = 1/3$ to $h = 2/3$ for the initial excited state with $m(k) = \theta(k - \pi/2)$. The four panels correspond to different distances, namely: a) $\ell = 20$, b) $\ell = 30$, c) $\ell = 60$, d) $\ell = 90$.

5.2 Analytical full time evolution for parity invariant states

In this section we provide an analytic result for the time dependence of the longitudinal two-point function for PIS and quenches within the ferromagnetic phase. For a quench starting from the ground-state and within the ferromagnetic phase, the two-point correlation function in the space-time scaling limit is [21, 24]

$$\rho^{xx}(\ell, t) \simeq C^x \exp \left[\ell \int_0^\pi \frac{dk}{\pi} \ln[|\cos \Delta_k|] \theta(2|\epsilon'_k|t - \ell) + 2t \int_0^\pi \frac{dk}{\pi} |\epsilon'_k| \ln[|\cos \Delta_k|] \theta(\ell - 2|\epsilon'_k|t) \right], \quad (84)$$

where $\theta(x)$ is the Heaviside step function and C^x is a coefficient which can also be calculated [24, 25]. This result is based on the multi-dimensional stationary phase approach developed in Refs. [17, 21, 24] and reported for completeness in Appendix A.

The derivation of Eq. (84) is based on the fact that the 2×2 symbol $\hat{\Gamma}(k)$ can be cast into the form (106) of Appendix A which, in particular, implies that the block symbol is

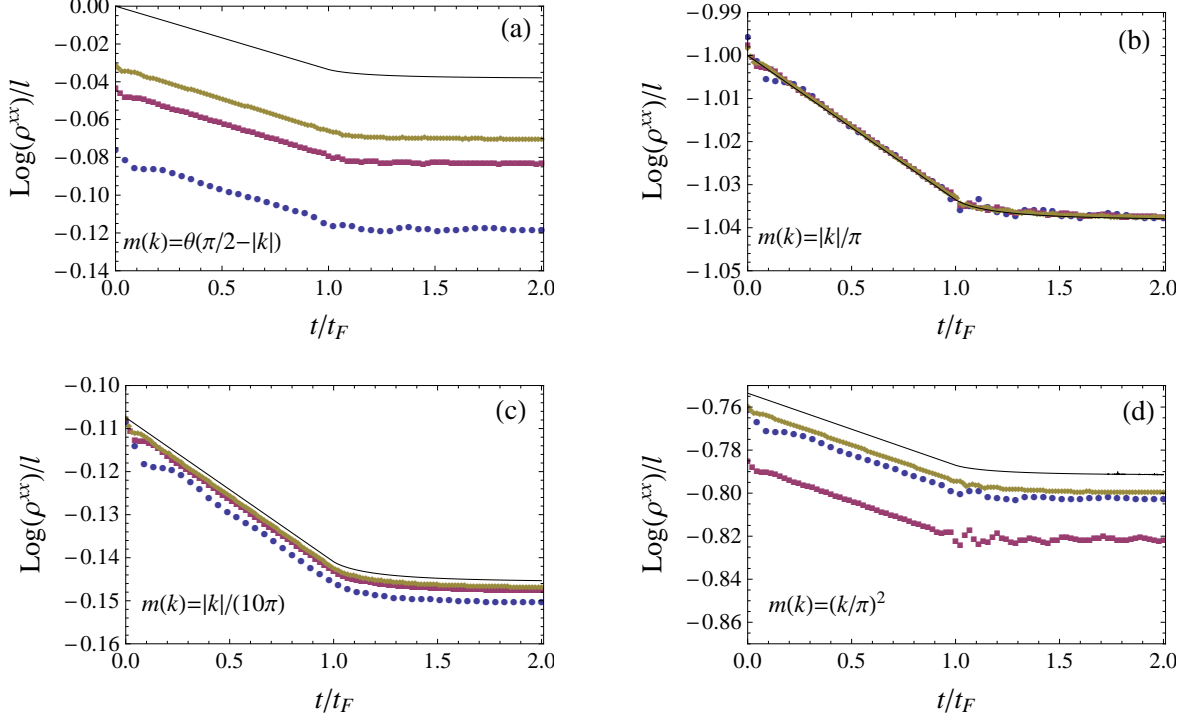


Figure 4: Scaling behaviour of $\ln(\rho^{xx})/\ell$ vs t/t_F . The continuous line is the analytical prediction in Eq. (88), the blue points correspond to $\ell = 30$, the violet squares to $\ell = 60$ and the dark green diamonds to $\ell = 90$. The various panels corresponds to different initial states with: a) $m(k) = \theta(\pi/2 - |k|)$, b) $m(k) = |k|/\pi$, c) $m(k) = |k|/(10\pi)$, d) $m(k) = (k/\pi)^2$.

traceless. The symbol for the excited state $\hat{\Gamma}^e(k)$ given in Eq. (80) is characterised by

$$\text{Tr}[\hat{\Gamma}^e(k)] = 2im_k^A, \quad \det[\hat{\Gamma}^e(k)] = (m_k^S)^2 - (m_k^A)^2 = (1 - 2m_k)(1 - 2m_{-k}). \quad (85)$$

Hence a generalised version of (84) can be derived only provided that the symbol is traceless, i.e. for PIS. In this case the symbol for the excited state is proportional to the one for the ground state $\hat{\Gamma}^{\text{gs}}(k)$, indeed from Eq. (80) we have

$$\hat{\Gamma}_{\text{PIS}}^e(k) = -m_k^S \hat{\Gamma}^{\text{gs}}(k), \quad (86)$$

and hence the coefficients n_x and \vec{n}_\perp appearing in Eq. (106) are

$$n_x = -m_k^S \cos \Delta_k, \quad |\vec{n}_\perp|^2 = \sin^2 \Delta_k (m_k^S)^2. \quad (87)$$

At this point, the generalisation of Eq. (84) to excited initial states is a straightforward

application of Eq. (108) in the appendix which leads to

$$\begin{aligned} \rho_{m_k}^{xx}(\ell, t) \simeq & C_{m_k} \exp \left[\ell \int_{-\pi}^{\pi} \frac{dk}{2\pi} \left(1 - 2|\epsilon'_k| \frac{t}{\ell} \right) \ln(|m_k^S|) \theta(\ell - 2|\epsilon'_k|t) \right] \\ & \exp \left[\ell \int_{-\pi}^{\pi} \frac{dk}{2\pi} \ln[|\cos \Delta_k m_k^S|] \theta(2|\epsilon'_k|t - \ell) \right] \\ & \exp \left[2t \int_{-\pi}^{\pi} \frac{dk}{2\pi} |\epsilon'_k| \ln[|\cos \Delta_k m_k^S|] \theta(\ell - 2|\epsilon'_k|t) \right]. \end{aligned} \quad (88)$$

Notice that compared with the ground state result there is an important qualitative difference given by the first line of the expression above that is absent only if $m_k = 0$ identically, i.e. for the ground state. In the multidimensional stationary phase approach this term arises from to the fact that $n_x^2 + |\vec{n}_\perp^2| \neq 1$. This term is also responsible for an exponential decay in the distance ℓ of the correlation function in the initial state, a fact that we anticipated in the previous section and that the above result proves.

In Fig. 4 we report the numerically calculated correlation functions and we compare with the analytic prediction (88). We plot the logarithm of the correlation in order to see clearly the exponential decay for $t < t_F$ followed by a slow relaxation for $t > t_F$. It is evident that increasing ℓ , the various curves approach the asymptotic result in Eq. (88). Finite size (in ℓ) effects are almost exclusively due to the undetermined constant C_{m_k} which in this kind of plots produces a ℓ^{-1} time-independent finite size correction, as proven by the fact that all curves are basically parallel. The behaviour of the state characterised by $m_k = (k/\pi)^2$ is a bit peculiar because increasing ℓ the numerical curves approach the analytic result in a non-monotonic way (the result for $\ell = 30$ is in between those for $\ell = 60$ and $\ell = 90$). This is not at all surprising because the coefficient C_{m_k} can depend on ℓ in an oscillating way every time that the symbol is a non-analytic function (for example in the long time limit the strong Szegő's lemma needs to be generalised to the Fisher–Hartwig formula, see e.g. [25] for explicit examples).

While in principle it is possible to compute the coefficient C_{m_k} for every excited states, each of them requires a different calculations and it is not worth analysing all of them. In order to give a typical example, in the next subsection we calculate this pre-factor for the state $m_k = k^2/(2\pi)^2$.

5.2.1 Computation of the pre-factor for an initial excited state

In this subsection we compute the coefficient C_{m_k} for the state $m_k = k^2/(2\pi)^2$. In general, the coefficient C_{m_k} can be extracted by evaluating it at infinite time when the matrix Γ becomes a standard time independent Toeplitz one and we can apply Szegő's lemma or generalisations (assuming that the space-time scaling limit and direct $t \rightarrow \infty$ commute, as it can be checked a posteriori). Calculations are largely simplified when the symbol is a smooth function and

the strong Szegő's lemma holds. For the cases explicitly reported in the previous subsection, this happens only for $m_k = k^2/(2\pi)^2$ and we will see that a closed form for C_{m_k} can indeed be found easily. On the contrary, for the other states examined above the symbol is not smooth and, as a consequence, generalisations of the Szegő's lemma are necessary, but since they require a case by case examination we prefer not to go into such details.

As shown in Refs. [25, 79], the strong Szegő's lemma gives the pre-factor C_{m_k} in the form

$$C_{m_k} = \exp \left[\sum_{q \geq 1} q (\ln t_\infty)_q (\ln t_\infty)_{-q} \right], \quad (89)$$

where $(\ln t_\infty)_q$ is the q -th coefficient of the Fourier expansion of the symbol at infinite time, i.e.

$$(\ln t_\infty)_q = \int_{-\pi}^{\pi} \frac{dk}{2\pi} (\ln t_\infty(e^{ik})) e^{-ikq}. \quad (90)$$

For $m(k) = k^2/(2\pi)^2$ we have

$$t_\infty(e^{ik}) = \cos \Delta_k \left(1 - \frac{k^2}{2\pi^2} \right), \quad (91)$$

and hence the Fourier coefficients are

$$(\ln t_\infty)_q = \begin{cases} \frac{h_0^q - 2h_1^{-q}}{2q} - \frac{2i\pi \sin(\pi q)}{\sqrt{2\pi q}}, & \text{if } q > 0, \\ \frac{2h_1^q - 2h^{-q} - h_0^{-q}}{2q} - \frac{2i\pi \sin(\pi q)}{\sqrt{2\pi q}}, & \text{if } q < 0, \end{cases} \quad (92)$$

where

$$h_1 = \frac{1 + hh_0 + \sqrt{(h^2 - 1)(h_0^2 - 1)}}{h + h_0}. \quad (93)$$

Computing the sum in Eq. (89), all the pieces depending on $\sin(\pi q)$ in (92) cancel, leading to

$$C_{m_k} = \frac{(h - h_1)(h_0 - h_1)}{\sqrt{1 - hh_0}(1 - h_0^2)^{1/4}(h_1^2 - 1)}. \quad (94)$$

Remarkably, this is independent on the specific value of $m(k)$ and it is indeed the same value obtained for the initial ground state [25]. In Fig. 5 we compare with the numerical results the full prediction for the time-dependent correlation function in Eq. (88) with the pre-factor given by Eq (94), hence with no unknown parameter. The agreement between the analytic formula and the numerics is excellent.

6 Time evolution of the entanglement entropy

In this section we turn to the study of the time evolution of the entanglement entropy of a block of ℓ contiguous spins after the quench from an excited state of the pre-quench Hamiltonian.

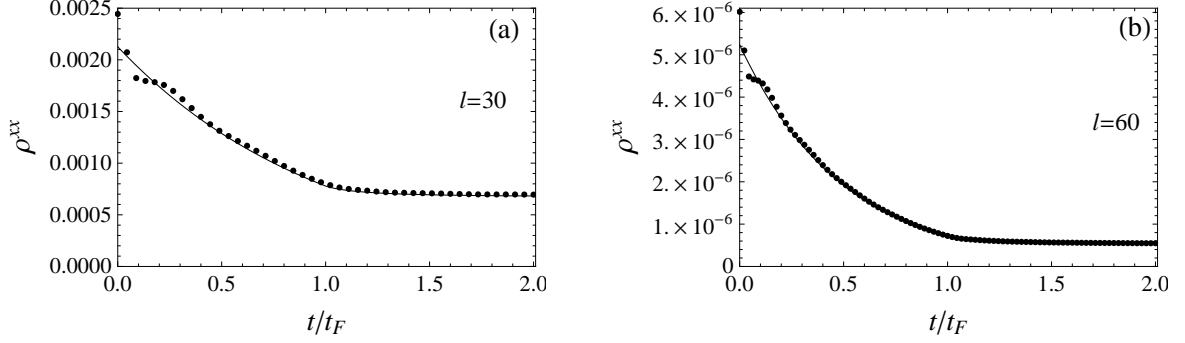


Figure 5: Time-dependent correlation function $\rho^{xx}(\ell, t)$ for the quench from $h_0 = 1/3$ to $h = 2/3$ with initial state given by $m(k) = k^2/(2\pi)^2$. The points are the numerical determination of the Pfaffian and the continuous line is the analytic prediction in Eq. (88) with pre-factor C_{m_k} fixed by Eq. (94). The two panels correspond to $\ell = 30$ (a) and $\ell = 60$ (b). The agreement is excellent in both cases.

As explained in Sec. 2.4, the time evolution of the entanglement entropy can be obtained from the eigenvalues of the correlation matrix Π in Eq. (32). For the case we are interested in the constituent blocks of this matrix have the form

$$\Pi_n = \begin{pmatrix} h_n & g'_n \\ -g'_{-n} & f_n \end{pmatrix}, \quad (95)$$

where f_n, h_n are the ones respectively given in Eq. (77) and Eq. (78), while g'_n turns out to be

$$g'_n = \int_{-\pi}^{\pi} \frac{dk}{2\pi} e^{ikn} [-m_k^S e^{i\theta(k)} (\cos \Delta_k - i \cos 2t\epsilon_k \sin \Delta_k)], \quad (96)$$

hence it differs from (79) by a factor e^{ik} .

By numerically calculating the eigenvalues of the matrix Π and inserting them in Eq. (37) we obtain a numerical estimate of the entanglement entropy.

6.1 Analytic evaluation of the entanglement entropy for parity invariant initial states

In this subsection we generalise the analytical formula which describes the time-dependence of the entanglement entropy of a block of spins of length ℓ after a quench starting from the ground state [16, 17], in the thermodynamic limit and in the limit of a large block $\ell \gg 1$. The leading behaviour in the space-time scaling limit for a quench from the ground state is [17]

$$S_A(t) = 2t \int_{2|\epsilon'_k|t < \ell} \frac{dk}{2\pi} |\epsilon'_k| H(\cos \Delta_k) + \ell \int_{2|\epsilon'_k|t > \ell} \frac{dk}{2\pi} H(\cos \Delta_k), \quad (97)$$

In the case of a traceless 2×2 symbol, i.e. for PIS, the generalisation of the aforementioned formula is direct using Eq. (108) in Appendix A. However, for NPIS a closed form cannot be obtained because the proof of the previous formula crucially relies on the tracelessness of the symbol.

Eq. (108) can be applied to the entanglement entropy since Eq. (37) is equivalent to

$$S = \text{Tr}[H[\Pi]], \quad (98)$$

where $H(x)$ is given in Eq. (37). Using Eq. (108) we have

$$\begin{aligned} \lim_{\substack{t, \ell \rightarrow \infty \\ t/\ell = \text{const}}} \frac{\text{Tr}[H[\Pi]]}{\ell} &= \int_{-\pi}^{\pi} \frac{dk}{2\pi} \max\left(1 - 2|\epsilon'_k| \frac{t}{\ell}, 0\right) H\left(\sqrt{n_x(k)^2 + |n_{\perp}(k)|^2}\right) + \\ &+ \int_{-\pi}^{\pi} \frac{dk}{2\pi} \min\left(2|\epsilon'_k| \frac{t}{\ell}, 1\right) H(n_x(k)). \end{aligned} \quad (99)$$

Inserting in this equation the explicit expressions for $n_x(k)$ and $n_{\perp}(k)$ in Eq. (87) we get, in the scaling limit, the entanglement entropy

$$\begin{aligned} S_A(\ell, t) &\simeq \int_{-\pi}^{\pi} \frac{dk}{2\pi} (\ell - 2|\epsilon'_k|t) H(m_k^S) \theta(\ell - 2|\epsilon'_k|t) + \\ &+ \ell \int_{-\pi}^{\pi} \frac{dk}{2\pi} H[m_k^S \cos \Delta_k] \theta(2|\epsilon'_k|t - \ell) + \\ &+ 2t \int_{-\pi}^{\pi} \frac{dk}{2\pi} |\epsilon'_k| H[m_k^S \cos \Delta_k] \theta(\ell - 2|\epsilon'_k|t). \end{aligned} \quad (100)$$

Also the entanglement entropy shows a light-cone behaviour, i.e. a linear growth for $t < t_F$ followed by a slow saturation. However, even in this case there is a main qualitative difference with the ground state result in Eq. (97) which is represented by the first line of the equation. This is again technically due to the fact that $n_x^2 + n_{\perp}^2 \neq 1$ and physically reflects the property that the entanglement entropy in the initial state is extensive. We mention that the zero time limit agrees with the results for the entanglement entropy found in Ref. [73] for the same class of excited states, but with a different method. Thus, for the entanglement entropy, the limit $t \rightarrow 0$ and the space-time scaling limit turn out to commute.

In order to show the correctness of our prediction, we report in Fig. 6 the numerical results for the entanglement entropy per spin starting from a few different parity invariant initial states which are compared with the analytic prediction (100). Increasing the size of the block of spins, the entanglement entropy obtained with the determinant approach gets closer and closer to the analytic formula. Being the various finite ℓ results all parallel to the

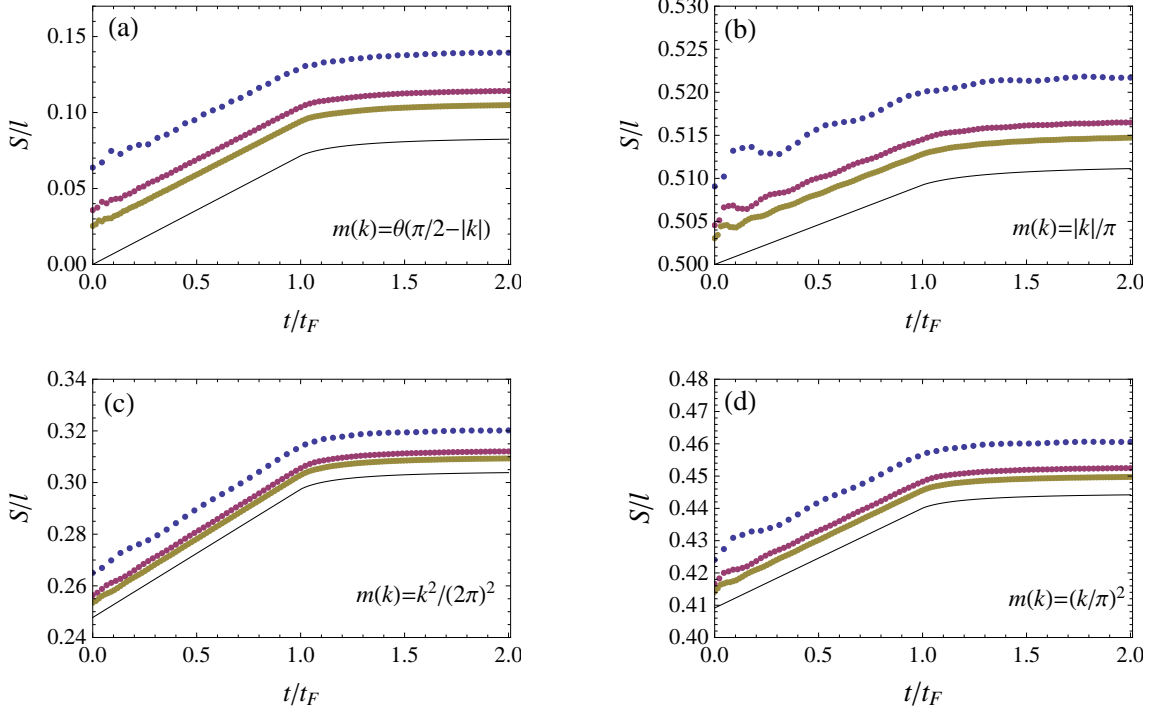


Figure 6: Time dependence of the entanglement entropy per spin starting from parity invariant states. The continuous line is the analytical formula Eq. (100), the blue points correspond to $\ell = 30$, the violet squares to $\ell = 60$ and the dark green diamonds to $\ell = 90$. (a) $m(k) = \theta(\pi/2 - |k|)$, (b) $m(k) = |k|/\pi$, (c) $m(k) = k^2/(2\pi)^2$, (d) $m(k) = (k/\pi)^2$.

prediction it is clear that the leading finite-size correction is just an additive constant which in principle could be obtained by means of Szegő's lemma or generalisations thereof.

In Fig. 7 we report the time evolution of the entanglement entropy per spin starting from non-parity invariant states. The light-cone spreading of the correlation is clear also in this case, but we do not have an analytic prediction. In order to exclude simple generalisations of Eq. (100), we also checked that the prediction for parity invariant states (using only the m_k^S part of the state) does not describe the numerical results.

6.2 Infinite time limit of the entanglement entropy

It is relatively easy to obtain the infinite time limit, not only for parity invariant states, but for an arbitrary initial state. Indeed, for infinite time, the entanglement entropy can be written as [16, 80]

$$S_A = \frac{1}{4\pi i} \oint d\lambda H(\lambda) \frac{d}{d\lambda} \ln D_\ell(\lambda), \quad D_\ell(\lambda) = \det(i\lambda I_\ell - \Pi_\ell), \quad (101)$$

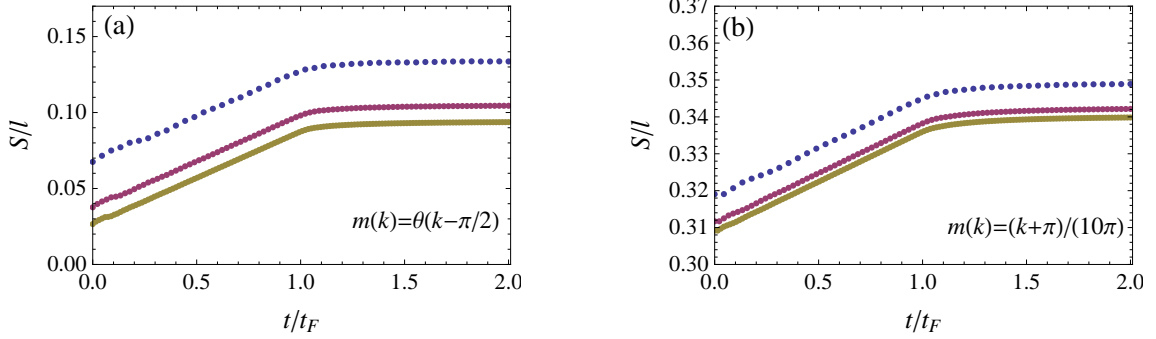


Figure 7: Time dependence of the entanglement entropy per spin for two non-parity invariant states. The blue dots correspond to $\ell = 30$, the violet ones to $\ell = 60$ and the dark green ones to $\ell = 90$. (a): $m(k) = \theta(k - \pi/2)$. (b): $m(k) = (k + \pi)/(10\pi)$.

where I_ℓ is the $2\ell \times 2\ell$ identity, $H(x)$ is defined in Eq. (37), and the integral is evaluated over a contour that encircles the segment $[-1, 1]$. The asymptotic (in ℓ) behaviour of $\ln D_\ell$ is found using a generalisation of Szegő's lemma [81]

$$\ln D_\ell(\lambda) = \frac{\ell}{2\pi} \int_{-\pi}^{\pi} dk \ln \left[\det \tilde{\Pi}(k) \right] + O(\ln \ell), \quad (102)$$

where

$$\tilde{\Pi}(k) = i\lambda I_1 - \Pi(k) = \begin{pmatrix} i\lambda - im_k^A & m_k^S e^{-i\theta(k)} \cos \Delta_k \\ -m_k^S e^{i\theta(k)} \cos \Delta_k & i\lambda - im_k^A \end{pmatrix}, \quad (103)$$

where $\Pi(k)$ is given by the infinite time limit of Eq. (33). Inserting the expression for $\det \tilde{\Pi}(k)$ in Eq. (102) and then in Eq. (101) we have the linear part in ℓ of the entanglement entropy

$$\begin{aligned} S_A(\ell, t = \infty) &\simeq \frac{\ell}{2\pi} \int_{-\pi}^{\pi} dk \frac{1}{4\pi i} \oint d\lambda H(\lambda) \frac{2(\lambda - m_k^A)}{(\lambda - m_k^A)^2 - (m_k^S)^2 \cos^2 \Delta_k} \\ &= \ell \int_{-\pi}^{\pi} \frac{dk}{2\pi} H(m_k^A + m_k^S \cos \Delta_k), \end{aligned} \quad (104)$$

where in the last line we first shifted the integral by m_k^A and then used the residue theorem. This is allowed because for arbitrary m_k we have $-1 < m_k^A + m_k^S \cos \Delta_k < 1$, where the function $H(x)$ is real. We stress that this is true for arbitrary states and not only for PIS. When specialised to PIS, the argument of the integral above reduces to $H(m_k^S \cos \Delta_k)$ which is the long time limit of Eq. (100) showing that for the entanglement entropy the scaling limit and the long time limit commute for arbitrary quenches.

7 Conclusions

We have considered the time evolution after a quench of the transverse magnetic field in the Ising model starting from an arbitrary excited state of the pre-quench Hamiltonian having the form

$$|\Psi_0\rangle = |m_k\rangle = \prod_k (b_k^\dagger)^{m_k} |0\rangle. \quad (105)$$

This state is fully specified by the characteristic function $m_k = 0, 1$ in finite systems, which in the thermodynamic limit becomes an arbitrary function $m(k)$ with $k \in [-\pi, \pi]$ and $m_k \in [0, 1]$. It turned out that important quantitative and qualitative differences in the time evolution arise between parity invariant initial states (i.e. with $m_k = m_{-k}$ for all k) and non parity invariant ones.

We showed that for an arbitrary state of the form (105) the long time limit of any local observable can be evaluated by means of GGE. The proof is based on the equivalence of two-point fermion correlations in the GGE and in the long time limit (taken, as usual, after the thermodynamic limit). Wick's theorem then allows for the construction of the full reduced density matrix of any finite block of spins and hence any local multi-point correlation. Although we limited ourself to the study of equal-time quantities, the general result of Ref. [26] allows us to conclude that the GGE describes also different times correlations.

Then we turned to the study of observables. We first considered the transverse magnetisation for which the non-parity invariance of the state does not play any role. We calculated the approach to the stationary value by means of the stationary phase approximation and we always found a power-law behaviour, but characterised by powers which depend on the initial state.

We then considered the two-point longitudinal correlation function at distance ℓ , since the one-point function vanishes for states of the form (105) even in the symmetry-broken phase. For parity invariant states and for quenches with the ferromagnetic phase, we found analytically the space-time scaling limit of this correlation by means of the multi-dimensional stationary phase approach. In all cases, the correlation function displays a typical light-cone feature with exponential relaxation for $t < t_F = \ell/2v_{\max}$ and slow relaxation for $t > t_F$. For non-parity invariant states, the numerical results show that the behaviour can be very different compared to the parity invariant counterpart and we still do not have a full understanding of the problem.

We also studied the entanglement entropy of a block of ℓ consecutive spins. We again found a light-cone spreading (i.e. linear increase followed by slow saturation) for arbitrary quenches and for arbitrary initial states. Also in this case, the space-time scaling limit is obtained analytically by means of the multi-dimensional stationary phase approach, but again only for parity invariant states. The infinite time limit has been derived for an arbitrary initial state, independently of its parity.

It is clearly an interesting open problem to understand the time-dependence of both the two-point correlation function and the entanglement entropy for non-parity invariant initial states. The different behaviour in these two classes of states could also be related to the fact that for non-parity invariant states the number of local conserved charges is doubled.

Acknowledgments

PC and MK acknowledge the ERC for financial support under Starting Grant 279391 ED-EQS. MK acknowledges financial support from the Marie Curie IIF Grant PIIF-GA-2012-330076. We thank Maurizio Fagotti for very fruitful discussions.

A The multidimensional stationary phase approximation

The evaluation of the correlation function $\rho^{xx}(\ell, t)$ and of the entanglement entropy $S_A(\ell, t)$ for large ℓ is equivalent to the asymptotic evaluation of the determinants and traces of a 2×2 block Toeplitz matrices, i.e. like Π and Γ in Eqs. (32) and (42). Several techniques like Szegő's lemma and the Fisher-Hartwig conjecture [79] permit the evaluation of traces/determinants of these matrices when the elements do not depend explicitly on the matrix size. This is in contrast to our case, where we are interested in the space-time scaling limit $\ell, t \rightarrow \infty$ with finite ratio ℓ/t . Thus, each element of the matrices Γ and Π in the space-time scaling limit depends on a parameter (namely t) which is proportional to the matrix dimension 2ℓ . This precludes the application of the aforementioned techniques, except for $t = 0$ and in the limit $t = \infty$. In order to deal with arbitrary large values of t , in Refs. [17, 21, 24] a new approach based on a multi-dimensional stationary phase approximation was developed. In this appendix we report the main result of Ref. [24] which has been extensively used in the text.

In Ref. [24] a very general result was obtained for any 2×2 -block Toeplitz matrix Λ with a symbol $\hat{t}(k)$ that can be cast in the form

$$\tilde{t}(k) = n_x(k)\sigma_x^{(k)} + \vec{n}_\perp(k) \cdot \vec{\sigma}^{(k)} e^{2i\epsilon(k)t\sigma_x^{(k)}}, \quad \vec{n}_\perp(k) \cdot \hat{x} = 0. \quad (106)$$

Here the time t is the only parameter proportional to the matrix size 2ℓ , n_x, n_\perp are fixed but otherwise arbitrary and $\sigma^{(k)}$ denotes a local rotation of the Pauli matrices

$$\sigma_\alpha^{(k)} \sim i e^{i\vec{w}(k) \cdot \sigma} \sigma_\alpha e^{-i\vec{w}(k) \cdot \sigma}. \quad (107)$$

All block symbols in Eq. (106) are traceless and have determinant equal to $n_x^2 + |\vec{n}_\perp|^2$.

Under the condition (106), the asymptotic value in the space-time scaling limit of the trace of an arbitrary analytic function $F(x)$ evaluated on the matrix Λ can be derived. The explicit result of Ref. [24] is

$$\lim_{\substack{t, \ell \rightarrow \infty \\ t/\ell \text{ const}}} \frac{\text{Tr}[F(\Lambda^2)]}{2\ell} = \int_{-\pi}^{\pi} \frac{dk_0}{2\pi} \max\left(1 - 2|\epsilon'(k_0)|\frac{t}{\ell}, 0\right) F(n_x(k_0)^2 + |n_\perp(k_0)|^2) + \\ + \int_{-\pi}^{\pi} \frac{dk_0}{2\pi} \min\left(2|\epsilon'(k_0)|\frac{t}{\ell}, 1\right) F(n_x(k_0)^2). \quad (108)$$

In this manuscript we applied this formula to the entanglement entropy and the longitudinal correlation. Indeed they can be written as functions of the matrices Π and Γ , respectively as

$$S_A = \text{Tr}(H[\Pi]), \quad (109)$$

$$\ln(\rho^{xx})^2 = \frac{1}{2}\text{Tr}(\ln \Gamma^2). \quad (110)$$

The function $H(x)$ is an analytic even function of x for $x \in (-1, 1)$ where the eigenvalues of Π lie, and so Eq. (108) can be applied with the only limitation that the symbol satisfies the constrain (106). The function $\ln(x^2)$ is instead non-analytic in $x = 0$ and this gives problems when the eigenvalues of Γ approach 0 in the thermodynamic limit. As discussed in Ref. [24], this problem limits the applicability of Eq. (108) to quenches within the ferromagnetic phase. For all the details about the limit of applicability of Eq. (108), we refer the reader to Ref. [24] and here we limit ourselves to the application of this form to cases in which it works.

A.1 A reduction formula

For the quench from the ground-state, in Ref. [24] it was very useful to reduce the determination of the Pfaffian of Γ to the determinant of an $\ell \times \ell$ matrix. Although we have not used it in this manuscript, it is worth mentioning that a similar formula holds also for the quench from excited states, but the new matrix is more complicated. Indeed, the spectral problem for a $2\ell \times 2\ell$ block Toeplitz matrix can be replaced by the spectral problem of an $\ell \times \ell$ Toeplitz + Hankel matrix

$$(iT \pm H)\vec{w}_k = \mp i\lambda_k \vec{w}_k, \quad (111)$$

where

$$\begin{aligned} T_{ij} &= \text{sign}(i-j)\sqrt{-h_{i-j}f_{i-j}}, \\ H_{ij} &= g_{i+j-\ell-1}. \end{aligned} \quad (112)$$

The matrix T is a Toeplitz matrix and the H has Hankel form. Hence we have

$$\rho^{xx}(\ell, t) = \text{pf}(\Gamma) = (-1)^{\frac{\ell(\ell-1)}{2}} \det(H + iT). \quad (113)$$

A similar reduction formula can be straightforwardly written down also for the matrix Π determining the entanglement entropy.

References

- [1] T. Kinoshita, T. Wenger, D. S. Weiss, *Nature* **440**, 900 (2006).
- [2] S. Trotzky Y.-A. Chen, A. Flesch, I. P. McCulloch, U. Schollwöck, J. Eisert, and I. Bloch, *Nature Phys.* **8**, 325 (2012).

- [3] M. Cheneau, P. Barmettler, D. Poletti, M. Endres, P. Schauss, T. Fukuhara, C. Gross, I. Bloch, C. Kollath, and S. Kuhr, *Nature* **481**, 484 (2012).
- [4] M. Gring, M. Kuhnert, T. Langen, T. Kitagawa, B. Rauer, M. Schreitl, I. Mazets, D. A. Smith, E. Demler, and J. Schmiedmayer, *Science* **337**, 1318 (2012).
- [5] U. Schneider, L. Hackermüller, J. P. Ronzheimer, S. Will, S. Braun, T. Best, I. Bloch, E. Demler, S. Mandt, D. Rasch, and A. Rosch, *Nature Phys.* **8**, 213 (2012).
- [6] A. Polkovnikov, K. Sengupta, A. Silva, and M. Vengalattore, *Rev. Mod. Phys.* **83**, 863 (2011).
- [7] P. Calabrese and J. Cardy, *Phys. Rev. Lett.* **96**, 136801 (2006).
- [8] P. Calabrese and J. Cardy, *J. Stat. Mech.* P06008 (2007).
- [9] E. H. Lieb and D. W. Robinson, *Commun. Math. Phys.*, **28**, 251 (1972).
- [10] A. Laeuchli and C. Kollath, *J. Stat. Mech.* (2008) P05018;
S. R. Manmana, S. Wessel, R. M. Noack, and A. Muramatsu, *Phys. Rev. B* **79**, 155104 (2009);
P. Barmettler, D. Poletti, M. Cheneau, and C. Kollath, *Phys. Rev. A* **85**, 053625 (2012).
- [11] J. M. Deutsch, *Phys. Rev. A* **43**, 2046 (1991);
M. Srednicki, *Phys. Rev. E* **50**, 888 (1994).
- [12] M. Rigol, V. Dunjko, V. Yurovsky, and M. Olshanii, *Phys. Rev. Lett.* **98**, 50405 (2007).
- [13] E. Barouch, B. McCoy, and M. Dresden, *Phys. Rev. A* **2**, 1075 (1970);
E. Barouch and B. McCoy, *Phys. Rev. A* **3**, 786 (1971)
E. Barouch and B. McCoy, *Phys. Rev. A* **3**, 2137 (1971).
- [14] F. Igloi and H. Rieger, *Phys. Rev. Lett.* **85**, 3233 (2000).
- [15] K. Sengupta, S. Powell, and S. Sachdev, *Phys. Rev. A* **69**, 053616 (2004).
- [16] P. Calabrese and J. Cardy, *J. Stat. Mech.* P04010 (2005).
- [17] M. Fagotti and P. Calabrese, *Phys. Rev. A* **78**, 010306 (2008).
- [18] A. Silva, *Phys. Rev. Lett.* **101**, 120603 (2008).
- [19] D. Rossini, A. Silva, G. Mussardo, and G. Santoro, *Phys. Rev. Lett.* **102**, 127204 (2009);
D. Rossini, S. Suzuki, G. Mussardo, G. Santoro, and A. Silva, *Phys. Rev. B* **82**, 144302 (2010).
- [20] F. Iglói and H. Rieger, *Phys. Rev. Lett.* **106**, 035701 (2011);
H. Rieger and F. Iglói, *Phys. Rev. B* **84**, 165117 (2011).
- [21] P. Calabrese, F.H.L. Essler, and M. Fagotti, *Phys. Rev. Lett.* **106**, 227203 (2011).
- [22] L. Foini, L. F. Cugliandolo, and A. Gambassi, *Phys. Rev. B* **84**, 212404 (2011);
L. Foini, L. F. Cugliandolo, and A. Gambassi, *J. Stat. Mech.* P09011 (2012).

- [23] D. Schuricht and F. H. L. Essler, J. Stat. Mech. P04017 (2012).
- [24] P. Calabrese, F.H.L. Essler, and M. Fagotti, J. Stat. Mech. P07016 (2012).
- [25] P. Calabrese, F.H.L. Essler, and M. Fagotti, J. Stat. Mech. P07022 (2012).
- [26] F. H. L. Essler, S. Evangelisti and M. Fagotti, Phys. Rev. Lett. **109**, 247206 (2012).
- [27] M. Fagotti and F.H.L. Essler, Phys. Rev. B **87**, 245107 (2013).
- [28] M. Fagotti, Phys. Rev. B **87**, 165106 (2013).
- [29] V. Gurarie, J. Stat. Mech. P02014 (2013).
- [30] M. Fagotti, ArXiv:1401.1064.
- [31] M. A. Cazalilla, Phys. Rev. Lett. **97**, 156403 (2006);
A. Iucci, and M. A. Cazalilla, Phys. Rev. A **80**, 063619 (2009);
A. Iucci, and M. A. Cazalilla, New J. Phys. **12**, 055019 (2010);
M. A. Cazalilla, A. Iucci, and M.-C. Chung, Phys. Rev. E **85**, 011133 (2012).
- [32] T. Barthel and U. Schollwöck, Phys. Rev. Lett. **100**, 100601 (2008).
- [33] M. Cramer, C. M. Dawson, J. Eisert, and T. J. Osborne, Phys. Rev. Lett. **100**, 030602 (2008);
M. Cramer and J. Eisert, New J. Phys. **12**, 055020 (2010).
- [34] S. Sotiriadis, P. Calabrese, and J. Cardy, EPL **87**, 20002 (2009).
- [35] J. Mossel and J.-S. Caux, New J. Phys. **14**, 075006 (2012).
- [36] M. Collura, S. Sotiriadis, and P. Calabrese, Phys. Rev. Lett. **110**, 245301 (2013);
M. Collura, S. Sotiriadis, and P. Calabrese, J. Stat. Mech. P09025 (2013).
- [37] M. Kormos, M. Collura, and P. Calabrese, Phys. Rev. A **89**, 013609 (2014).
- [38] M. Rajabpour and S. Sotiriadis, arXiv:1307.7697.
- [39] M. Collura, M. Kormos, and P. Calabrese, J. Stat. Mech. P01009 (2014).
- [40] J.-S. Caux and F.H.L. Essler, Phys. Rev. Lett. **110**, 257203 (2013).
- [41] D. Fioretto and G. Mussardo, New J. Phys. **12**, 055015 (2010).
- [42] B. Pozsgay, J. Stat. Mech. P01011 (2011).
- [43] J. Mossel and J.-S. Caux, J. Phys. A **45**, 255001 (2012);
E. Demler and A. M. Tsvelik, Phys. Rev. B **86**, 115448 (2012).
- [44] J.-S. Caux and R. M. Konik, Phys. Rev. Lett. **109**, 175301 (2012).
- [45] S. Sotiriadis, D. Fioretto, and G. Mussardo, J. Stat. Mech. P02017 (2012).

- [46] M. Fagotti and F.H.L. Essler, *J. Stat. Mech.* P07012 (2013).
- [47] B. Pozsgay, *J. Stat. Mech.* P07003 (2013).
- [48] M. Kormos, A. Shashi, Y.-Z. Chou, J.-S. Caux and A. Imambekov, *Phys. Rev. B* **88**, 205131 (2013).
- [49] G. Mussardo, *Phys. Rev. Lett.* **111**, 100401 (2013).
- [50] B. Pozsgay, arXiv:1309.4593.
- [51] M. Fagotti, arXiv:1308.0277; B. Pozsgay, arXiv:1308.3087.
- [52] J. De Nardis, B. Wouters, M. Brockmann, and J.-S. Caux, arXiv:1308.4310.
- [53] D. Iyer and N. Andrei, *Phys. Rev. Lett.* **109**, 115304 (2012);
D. Iyer, H. Guan, and N. Andrei, *Phys. Rev. A* **87**, 053628 (2013);
W. Liu and N. Andrei arXiv:1311.1118.
- [54] S. Sotiriadis, G. Takacs, and G. Mussardo, arXiv:1311.4418.
- [55] M. Brockmann, J. De Nardis, B. Wouters, and J.-S. Caux, arXiv:1401.2877.
- [56] M. Fagotti, M. Collura, F. H. L. Essler, and P. Calabrese, arXiv:1311.5216.
- [57] C. Kollath, A. Laeuchli, and E. Altman, *Phys. Rev. Lett.* **98**, 180601 (2007).
- [58] M. Rigol, V. Dunjko, and M. Olshanii, *Nature* **452**, 854 (2008).
- [59] M. Rigol, *Phys. Rev. Lett.* **103**, 100403 (2009); *Phys. Rev. A* **80**, 053607 (2009);
M. Rigol and M. Fitzpatrick, *Phys. Rev. A* **84**, 033640 (2011);
K. He and M. Rigol, *Phys. Rev. A* **85**, 063609 (2012).
- [60] G. Roux, *Phys. Rev. A* **79**, 021608 (2009);
G. Roux, *Phys. Rev. A* **81**, 053604 (2010).
- [61] G. Biroli, C. Kollath, and A.M. Läuchli, *Phys. Rev. Lett.* **105**, 250401 (2010).
- [62] M. C. Banuls, J. I. Cirac, and M. B. Hastings, *Phys. Rev. Lett.* **106**, 050405 (2011).
- [63] A. C. Cassidy, C. W. Clark, and M. Rigol. *Phys. Rev. Lett.* **106**, 140405 (2011).
- [64] G. P. Brandino, A. De Luca, R. M. Konik, and G. Mussardo, *Phys. Rev. B* **85**, 214435 (2012).
- [65] E. Canovi, D. Rossini, R. Fazio, G. Santoro, and A. Silva, *New J. Phys.* **14**, 095020 (2012).
- [66] M. Rigol and M. Srednicki, *Phys. Rev. Lett.* **108**, 110601 (2012).
- [67] J. Sirker, N.P. Konstantinidis, and N. Sedlmayr, arXiv:1303.3064.
- [68] T. M. Wright, M. Rigol, M. J. Davis, K. V. Kheruntsyan, arXiv:1312.4657.

- [69] M. Rigol, arXiv:1401.2160.
- [70] F. H. L. Essler, S. Kehrein, S. R. Manmana, and N. J. Robinson, arXiv:1311.4557.
- [71] J. Eisert, M. Cramer, and M. B. Plenio, *Rev. Mod. Phys.* **82**, 277 (2010).
- [72] J. I. Cirac and F. Verstraete *J. Phys.* **42**, 504004 (2009);
U. Schollwök, *Ann. Phys.* **326**, 96 (2011);
P. Hauke, F. M. Cucchietti, L. Tagliacozzo, I. Deutsch, and M. Lewenstein, *Rep. Progr. Phys.* **75**, 082401 (2012).
- [73] V. Alba, M. Fagotti, and P. Calabrese, *J. Stat. Mech.* P10020 (2009).
- [74] S. Sachdev, *Quantum Phase Transitions*, Cambridge University Press, 2001.
- [75] G. Vidal, J. I. Latorre, E. Rico, and A. Kitaev, *Phys. Rev. Lett.* **90**, 227902 (2003);
J. I. Latorre, E. Rico, and G. Vidal, *Quant. Inf. and Comp.* **4**, 048 (2004).
- [76] I. Peschel and V. Eisler, *J. Phys. A* **42**, 504003 (2009).
- [77] M. Fagotti and P. Calabrese, *J. Stat. Mech.* P04016 (2010).
- [78] T. Prosen, *J. Phys. A* **31**, L97 (1998).
- [79] P. Deift, A. Its, and I. Krasovsky, *Ann. Math.* **174**, 1243 (2011);
A. Boettcher and H. Widom, *Lin. Alg. Appl.*, **419**, 656 (2006).
- [80] B.-Q. Jin and V. E. Korepin, *J. Stat. Phys.* **116**, 79 (2004);
P. Calabrese and F. H. L. Essler, *J. Stat. Mech.* P08029 (2010).
- [81] H. Au-Yang and B. McCoy, *Phys. Rev. B* **10**, 3885 (1974).